INTRAPARTICLE DIFFUSION[1]

In this chapter we look into sorption/desorption kinetics limited by intraparticle pore diffusion, i.e. porous particles (rock fragments, chars, activated carbon) or clay aggregates.

1. THE SPHERICAL DIFFUSION MODEL

Solute diffusion into soil aggregates, lithofragments or other particles in sediments and aquifer materials in the sorptive uptake and desorption mode may be described with Fick´s second law in spherical coordinates:

$$\frac{\partial C}{\partial t} = D_a \left[\frac{\partial^2 C}{\partial r^2} + \frac{2}{r} \frac{\partial C}{\partial r} \right] \qquad (1.1)$$

where C, t and r denote concentration [M L^{-3}], time and the radial distance [L] from the center of the sphere. For constant D_a (e.g. linear sorption isotherms) and a variety of initial and boundary conditions analytical solutions of eq. 1.1 are available. They allow the calculation of the solute mass in the sphere after a time t as well as the sorption and desorption rates.

$$\frac{\partial C}{\partial t} = D_a \left[\frac{\partial^2 C}{\partial r^2} + \frac{2}{r} \frac{\partial C}{\partial r} \right]$$

... in spherical coordinates
(for sand, gravel, rocks ...)

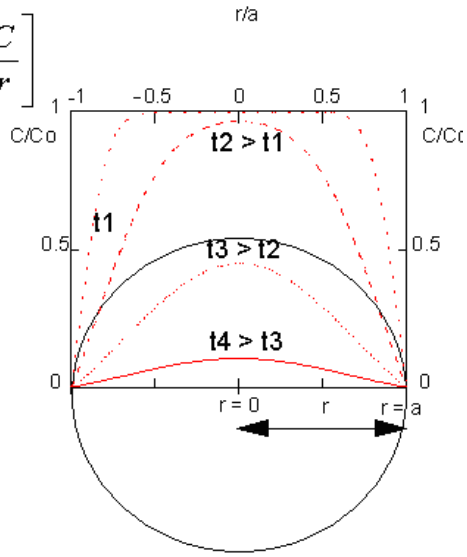

Fig. 1.1: Solute diffusion out of a sphere. Concentration profiles after times t1 – t4. a is the radius of the sphere and r the radial distance (coordinate) from the center. D_a is the apparent diffusion coefficient in a porous medium defined as the effective diffusion coefficient D_a divided by the capacity factor ($\varepsilon + K_d \rho_b$).

$$\frac{C}{C_0} = 1 + \frac{2a}{\pi r} \sum_{n=1}^{\infty} \frac{(-1)^n}{n} \sin\left[\frac{n\pi r}{a}\right] \exp\left[\frac{-n^2 \pi^2 D_a t_e}{a^2}\right]$$

Note, that in this chapter we use "a" to denote the radius of a sphere ("r" denotes here radial distance from the center of the sphere)

[1] Parts of this chapter comes to a large extent from the book: Diffusion in Natural Porous Media: Contaminant Transport, Sorption/Desorption and Dissolution Kinetics. Kluwer Academic Publishers, Boston, 224 p. (ISBN 0-7923-8102-5); Peter Grathwohl, 1998

1.1 DIFFUSION LIMITED SORPTIVE UPTAKE AND DESORPTION (INFINITE BATH)

The mass which has diffused into or out of the solid (sorbed or desorbed) after time t (here denoted: M) relative to the mass which sorbed or desorbed after equilibrium was achieved (M_{eq}) is given as (Crank, 1975):

$$\frac{M}{M_{eq}} = 1 - \frac{6}{\pi^2}\sum_{n=1}^{\infty}\frac{1}{n^2}\exp\left[-n^2\pi^2\frac{D_a}{a^2}t\right] \tag{1.2}$$

The term $D_a\,t/a^2$ denotes the dimensionless time which is also known as Fourier number. M_{eq} may be expressed as the concentration [M M^{-1}] or the absolute mass per sphere [M] based on the aqueous concentration at equilibrium C_{eq} [M L^{-3}]:

$$M_{eq} = C_{eq}\frac{\alpha}{\rho_p} = \frac{C_{eq}}{\rho_p}\left(\varepsilon + K_d\rho_p\right) \tag{1.3a}$$

or

$$M_{eq} = C_{eq}\left(\varepsilon + K_d\rho_p\right)\frac{4}{3}\pi a^3 \quad [\mathrm{M}/sphere] \tag{1.3b}$$

ε and ρ_p are the porosity and bulk density of the particle (pore volume and solid mass per total volume of the particle). The diffusion rate to and from the sphere (the solute flux across the surface of the sphere) corresponding to Eq. 1.2 is given by the time derivative:

$$\frac{F}{M_{eq}} = \frac{D_a}{a^2}6\sum_{n=1}^{\infty}exp\left[-n^2\pi^2\frac{D_a}{a^2}t\right] \tag{1.4}$$

The units of F depend on the definition of M_{eq} (eq. 1.3a, b), e.g., mass of solute per time and mass of solids [M t^{-1} M^{-1}] or flux [M t^{-1}] based on a single sphere. Since F depends on M_{eq} (= $C_{eq}\,\alpha/\rho_p$; eq. 1.3), the rates of sorption or desorption increase with an increasing capacity factor or sorption coefficient K_d, respectively. For long periods of time ($D_a\,t\,/\,a^2 > 0.05$) the first term in eq. 1.2 and 1.4 sufficiently estimates the desorption times and the corresponding fluxes. M/M_{eq} is then simply (long-term approximation for n = 1 in the series expansions):

$$\frac{M}{M_{eq}} = 1 - \frac{6}{\pi^2}\exp\left[-\pi^2\frac{D_a}{a^2}t\right] \tag{1.5}$$

The long-term approximation for the diffusive flux (e.g., the desorption rate) is:

$$\frac{F}{M_{eq}} = 6\frac{D_a}{a^2}\exp\left[-\pi^2\frac{D_a}{a^2}t\right] \tag{1.6}$$

These long-term approximations (eqs. 1.5 and 1.6) show that for long periods of time diffusion is analogous to first order reaction kinetics resulting in a slope of ($-\pi^2 D_a\,/a^2$) in a semi-logarithmic plot (log F *vs.* t).

For short time periods a large number of terms is necessary in the series expansions of eqs. 1.3 and 1.4 (see Figure 1.7 for $D_a\,t/a^2$ < 1E-04). If $D_a\,t\,/a^2 < 0.15$ or M/M_{eq} =0.95, the following short-term approximations may be used for estimating the mass sorbed or desorbed after a certain time and the corresponding diffusive fluxes:

$$\frac{M}{M_{eq}} = 6\sqrt{\frac{D_a t}{\pi a^2}} - 3\frac{D_a t}{a^2} \tag{1.7}$$

$$\frac{F}{M_{eq}} = 3\sqrt{\frac{D_a}{\pi a^2}}\frac{1}{\sqrt{t}} - 3\frac{D_a}{a^2} \tag{1.8}$$

For short time periods with $D_a t/a^2 < 0.01$, the last terms in eqs. 1.7 and 1.8 can be dropped, M/M_{eq} and F depend solely on the square root of time. Figures 1.7 and 1.8 show the analytical solutions and compare the short and long-term approximation. The time required for the sorption or desorption of a specific, high fraction (e.g., > 60%) of the contaminant can be calculated easily from the long-term approximation for M/M_{eq} (eq. 1.5):

$$\mathrm{t} = \left(-0.233\log\left[1 - \frac{M}{M_{eq}}\right] - 0.05\right)\frac{a^2}{D_a} \tag{1.9}$$

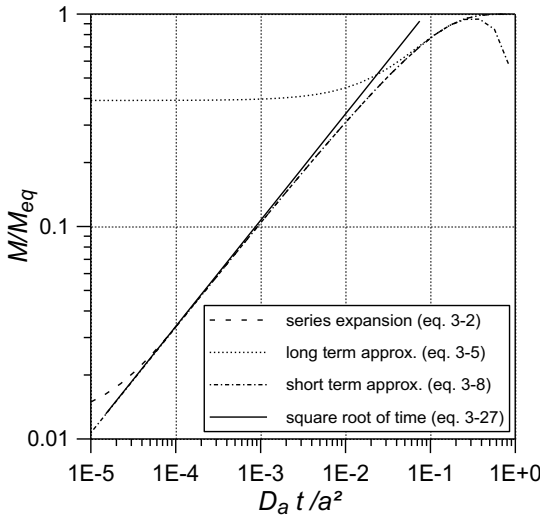

Fig. 1.2: Analytical solution (50 terms in Eq. 1.2) as well as short and long-term approximations of M/M_{eq} in an infinite bath (constant surface concentration, equilibrium at t = 0)

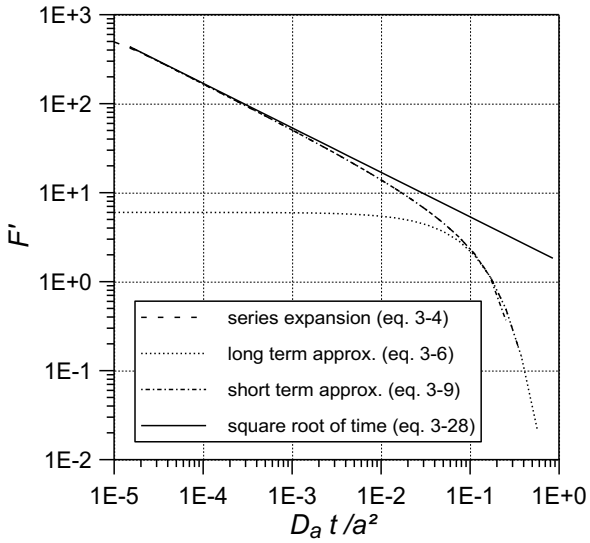

Fig. 1.3: Analytical solution (128 terms in Eq. 1.4) as well as short and long-term approximations of F in an infinite bath (constant surface concentration). F' denotes normalized flux expressed as $F/(M_{eq}\, D_a/a^2)$

1.2 COMPARISON OF SPHERICAL TO NON-SPHERICAL GEOMETRIES

Particles in soils and sediments may deviate from a spherical shape, especially shale fragments, clay aggregates (also clay minerals) or microporous crystals such as zeolites. In the following section analytical solutions for M/M_{eq} and the corresponding fluxes in an infinite bath for spherical sorbent geometry are compared to cylindrical, plane and cubic geometries. At short periods the sorptive uptake or the desorption rates are independent of the geometry and solely depend on the surface to volume ratio of the particle.

The short-term approximations for the different geometries discussed above are equivalent, based on the ratios of an external surface area to the volume A/V [L^2L^{-3}]:

$$\begin{aligned}\frac{A}{V} &= \frac{3}{a} \text{ for a } sphere\\ &= \frac{2}{a} \text{ for a } cylinder\\ &= \frac{2}{d} \text{ for a plane } sheet\\ &= 2\left(\frac{1}{b}+\frac{1}{c}+\frac{1}{d}\right) \text{ for a } parallelepiped\\ &= \frac{6}{c} \text{ for a } cube\end{aligned} \tag{1.10}$$

Short-term approximations of M/M_{eq} for particles of different geometries may be calculated provided A/V is known:

$$\frac{M}{M_{eq}} = \frac{2A}{V}\sqrt{\frac{D_a t}{\pi}} \tag{1.11}$$

The corresponding diffusive fluxes are simply given by the time derivative of Eq.1.11:

$$\frac{F}{M_{eq}} = \frac{A}{V}\sqrt{\frac{D_a}{\pi t}} \tag{1.12}$$

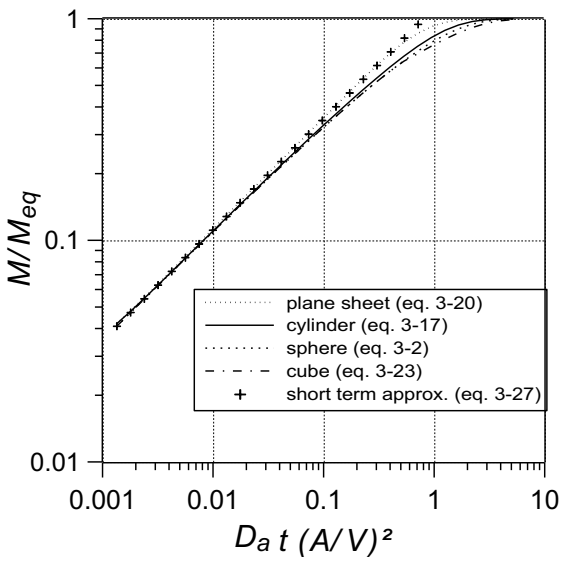

Fig. 1.4: Influence of shape on M/M_{eq} versus dimensionless time (infinite bath)

Figure 1.4 shows a comparison of M/M_{eq} of the different geometries discussed above. Since diffusion at short time scales is a process depending essentially on the surface to volume ratio of the particle - the shape, as well as particle size distributions, do not influence influence the diffusive fluxes much. However, if the long-term behavior is considered, the differences between the various geometries become more pronounced. Figures 1.4 and 1.5 show that the sorption/desorption rates (diffusive fluxes) in a slab (plane sheet) decline faster than the other geometries. Diffusion in a cube, with the longest diagonal distance from the edges to the center appears slower than diffusion in a cylinder or sphere (based on the ratio A/V).

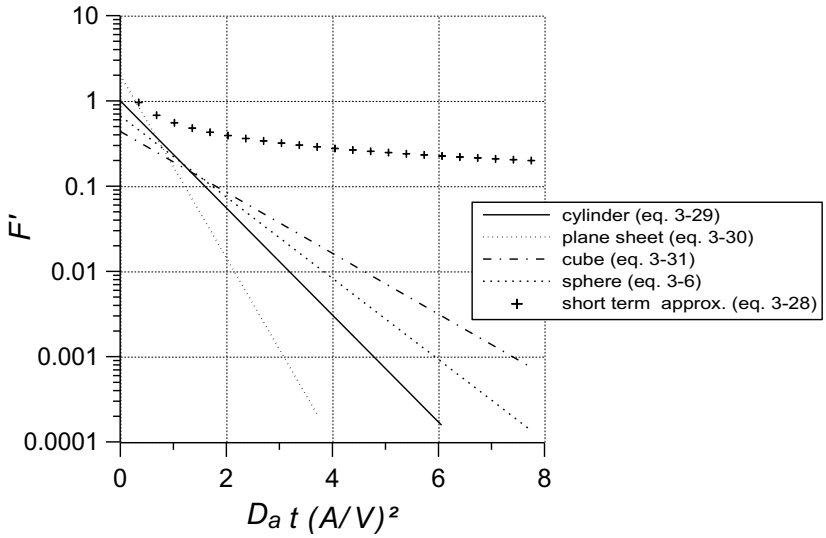

Fig. 1.5: Influence of shape on diffusive fluxes (semi-log plot) versus dimensionless time (a long-term approximation for the infinite bath)

1.3 NONLINEAR SORPTION: NUMERICAL MODELING OF SPHERICAL DIFFUSION

Numerical simulation of diffusion-controlled sorption/desorption may become necessary if the initial conditions for the analytical solutions presented above are not met (e.g., changing concentrations at the interface between the immobile and the mobile phase). Furthermore, the analytical solutions are only valid for constant diffusion coefficients, requiring linear sorption isotherms. However, sorption of hydrophobic compounds in soils and sediments often exhibits nonlinearity especially when large concentration ranges (in q and C) are involved. For most Freundlich isotherms in soils, the relative sorption capacity (expressed as K_d) decreases with increasing solute concentration (Freundlich exponent: $1/n < 1$). This results in concentration-dependent diffusion coefficients, e.g. decreasing D_a with decreasing concentration. During desorption, when concentrations decrease by orders of magnitude, D_a may increase by a factor of ten or more depending on $1/n$. In these cases, a numerical solution of eq. 1.1 is necessary in order to calculate M/M_{eq} and F.

For nonlinear Freundlich type isotherms, D_a is obtained from the derivative of the Freundlich isotherm:

$$D_a = \frac{D_e}{\varepsilon + K_{Fr}\rho_p \, {}^1\!/_n \, C^{{}^1\!/_{n-1}}} \tag{1.13}$$

In the nonlinear case, the sorption and desorption curves are different, especially if $1/n$ is smaller than 0.7. Therefore, nonlinear sorption isotherms cause "*hysteresis*" of the sorption/desorption

kinetics (hysteresis results in different sorption compared to desorption curves). With an increasing degree of nonlinearity, the sorption rate increases faster than the desorption rate (Kärger and Ruthven, 1992). Therefore, an asymmetry develops between sorption and desorption (Figure 1.6) which is entirely an effect of nonlinear sorption isotherms (e.g. there is no difference in pore diffusion coefficient during sorption and desorption). It may be compared with a self-sharpening front and tailing of a peak in chromatography or advective transport of a reactive tracer in groundwater with nonlinear sorption isotherms ($1/n < 1$). The asymmetry (hysteresis) between adsorption and desorption of organic vapors (benzene, TCE) and water from dry soils was well resolved using concentration-dependent diffusion coefficients (Shonnard et al, 1993; Lin et al., 1994).

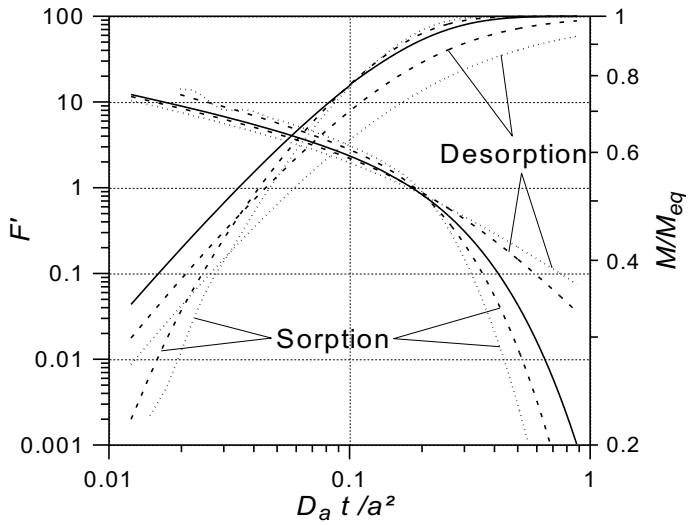

Fig. 1.6: Influence of nonlinear Freundlich type sorption isotherms on F (descending curves, left axis) and M/M_{eq} (ascending curves, right axis) during sorption and desorption (C_{eq} = 1). Solid lines. Linear case (sorption matches desorption); dashed lines: 1/n = 0.7; dotted lines: 1/n = 0.5; $F' = F/(M_{eq}D_a/a^2)$; D_a at C = 1.

1.4 NON-UNIFORM CONCENTRATION DISTRIBUTIONS

If the sorption of organic compounds in soils and sediments is very slow (e.g. if it takes decades to reach equilibrium), desorption during remediation may start before a uniform concentration of the solute in the sorbing particles or aggregates (sorption equilibrium) has been attained. This also applies to many bench-scale desorption studies that equilibrium was not established before starting the elution experiment. In these cases, at the beginning of the desorption process, concentration gradients exist in both directions: towards the center and towards the surface of the particle. At early times, therefore, a fraction of the solute still diffuses in the direction of the center of the particle.

Box 1.1. Numerical solution for the spherical diffusion model

Here, a simple explicit finite difference model is described to discuss the influence of nonlinear sorption isotherms on sorption and desorption kinetics. Wu and Gschwend (1988) used a similar approach to simulate sorption kinetics in particle mixtures of different sizes. For more elaborate methods see Crank (1975) or Fong and Mulkey (1990). Eq. 1.1 is expressed in finite differences as follows:

$$D_a \frac{\partial^2 C}{\partial r^2} = \frac{D_a}{\Delta r^2}\left(C_{j+1} - 2C_j + C_{j-1}\right) \quad \text{and:} \quad \frac{D_a}{r}\frac{2}{}\frac{\partial C}{\partial r} = \frac{D_a}{r\Delta r}\left(C_{j+1} - C_{j-1}\right)$$

C_j denotes the solute concentration in the pore water at node j. Combining both parts and setting $r = j$ Dr yields:

$$D_a\left[\frac{\partial^2 C}{\partial r^2} + \frac{2}{r}\frac{\partial C}{\partial r}\right] = \frac{D_a}{\Delta r^2}\left[\left(1 + \frac{1}{j}\right)C_{j+1} - 2C_j + \left(1 - \frac{1}{j}\right)C_{j-1}\right]$$

The concentration after time step k+1 at each grid point $C_j^{k\square 1}$ may then be calculated from the concentrations at the previous time step (C_j^k):

$$C_j^{k+1} = D_a \frac{\Delta t}{\Delta r^2}\left[\left(1 + \frac{1}{j}\right)C_{j+1}^k - 2C_j^k + \left(1 - \frac{1}{j}\right)C_{j-1}^k\right] + C_j^k$$

The initial and boundary conditions are satisfied by setting the appropriate concentrations at time zero and the interface, respectively. For the innermost node (j = 0) the concentration gradient is always zero ($\partial C/\partial r$ = 0).

This explicit numerical solution is easily implemented in a spreadsheet. It allows for calculating the concentration profiles in the sphere at given time (see example at end of this chapter - Fig. 3.25). The dimensionless group $D_a \Delta t/\Delta r^2$ has to be smaller than 0.5 to avoid oscillations and instabilities. The accuracy depends on the grid number while the errors increase with decreasing dimensionless time. To reduce the errors at $D_a t/a^2 > 0.01$ to less than 10% a grid number of 9 is sufficient (Fig. 3.9).

The solute mass in the sphere (M_S) at a given time is given by:

$$M_s = \frac{4\pi}{3}\left(\varepsilon + K_d\rho_p\right)\sum_{j=0}^{m}\left(r_{j+1}^3 - r_j^3\right)\frac{\left(C_j + C_{j+1}\right)}{2}$$

For nonlinear Freundlich type isotherms, if 1/n < 1, D_a decreases with decreasing solute concentrations in the intraparticle pores. This results in a decreasing "time-dependent" D_a during desorption. K_d in the above equation for a Freundlich isotherm may be calculated from:

$$K_d = K_{Fr}\left(\frac{C_j + C_{j+1}}{2}\right)^{1/n-1}$$

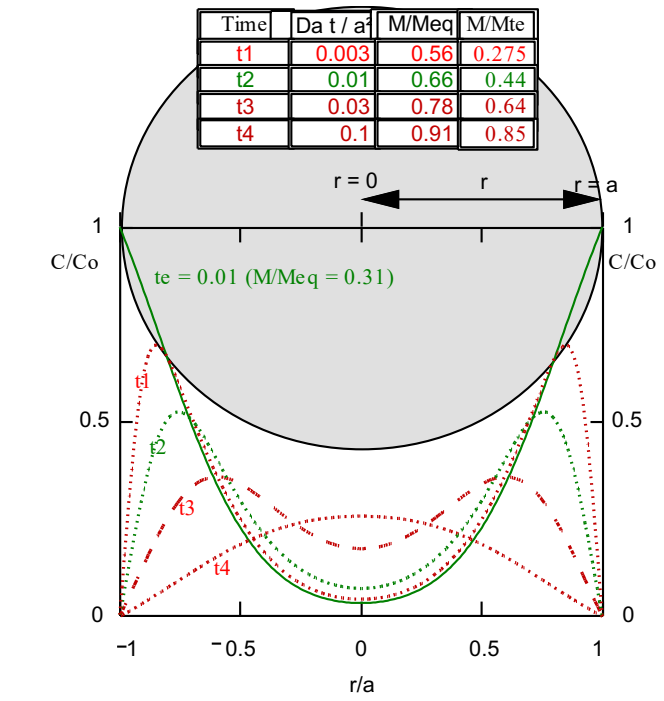

Fig. 1.7: Concentration profiles in a sphere if desorption is started before sorption equilibrium is reached. Solid line: concentration after exposure for $D_a\ t/a^2$ = 0.05; dashed lines: concentration profiles during desorption.

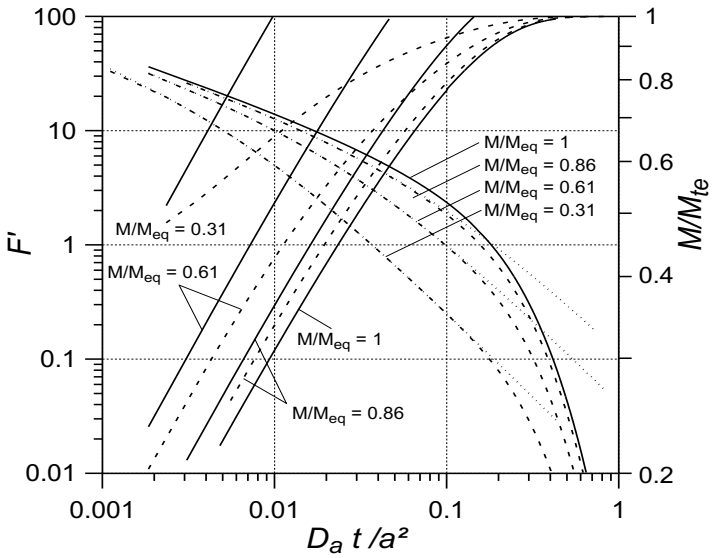

Fig. 1.8: F´(descending lines, left) and M/M_{te} (ascending lines, right) after different initial degrees of equilibration: M/M_{eq} = 0.31, 0.61, 0.86, and 1 (equilibrium) corresponding to $D_a\ t_e/a^2$ of 0.01, 0.05, 0.15, and ∞ (sorption equilibrium) respectively. Solid lines: sorption; dashed lines: desorption; dotted lines: short-term approximations $F´=F/(M_{eq}D_a/a^2)$

1.5 SORPTION/DESORPTION DYNAMICS IN HETEROGENEOUS MATERIALS

Many aquifer materials consist of a variety of components and grains of different sizes and therefore represent a chemically and physically heterogeneous mixture. The components are minerals (e.g. quartz, clay minerals) and fragments of rocks (e.g. limestones, sandstones, mudstones, shales, etc.). In a mixture of grains of different size, different sorption capacity and porosity, a single diffusion rate constant cannot describe the diffusion of a solute into or out of all the grains. The analytical solutions for diffusion-limited sorption and desorption as discussed above are only valid for a mixture of particles with a size distribution that is within one order of magnitude (Wu and Gschwend, 1986; Mathews and Zayas, 1989). Therefore, each component i with diffusion coefficients $D_{a,i}$ and grain radius a_i has to be considered.

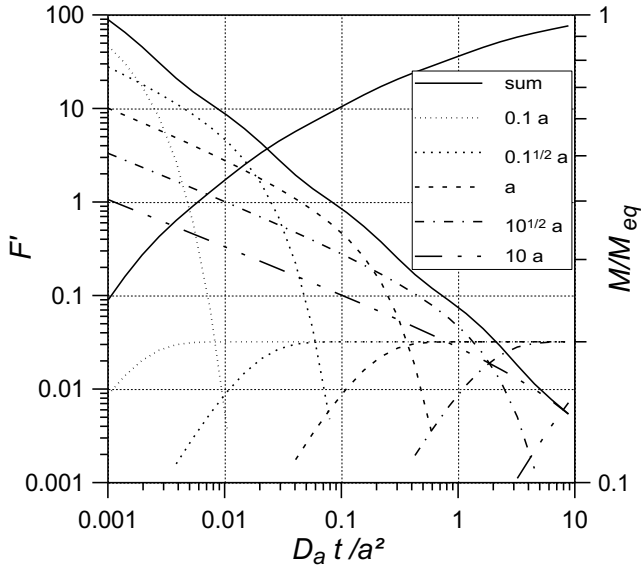

Example for D_a = 1x10^{-10} [cm^2 s^{-1}]:

Component	Fraction	a [cm^2]	$D_a\, a^{-2}$ [s^{-1}]
1	0.2	0.01	1x10^{-6}
2	0.2	0.0316	1x10^{-7}
3	0.2	0.1	1x10^{-8}
4	0.2	0.316	1x10^{-9}
5	0.2	1	1x10^{-10}

Fig. 1.9: Contributions of 5 components (equally distributed, each sorbing 20% of the sorbate, X_i = 0.2) to F' (descending curves) and M/M_{eq} (ascending curves) for a hypothetical mixture with D_a/a^2 spanning over 5 orders of magnitude (e.g. the grain radius varies over 3 orders of magnitude: between 1/10 and the 10 fold of the mean). Normalization of F' and time are based on the geometric mean of D_a/a^2.

Figure 1.9 shows M/M_{eq} and F' calculated for an exemplary mixture of 5 components, each making up for 20% (X_i = 0.2) of the equilibrium sorptive uptake of the bulk with diffusion rate constants ranging over five orders of magnitude (e.g. 0.00001, 0.0001, 0.001, 0.01, 0.1 s^{-1}). In this heterogeneous mixture of particles, the curves of log F and log M/M_{eq} versus log time deviate substantially from the curves predicted for diffusion in a homogeneous sample. The slope of F almost approaches -1 as opposed to -0.5 as predicted for short-term diffusion. When the diffusion rate constants cover a smaller range, the deviation from the monodisperse case is less prominent.

The theoretical results show that when M/M_{eq} becomes smaller than approximately 0.2, the curves for various normal and log-normal particle size distributions (or distributions of D_a/a^2, respectively) begin to diverge significantly. If a broad distribution of D_a/a^2 (or a) is given (Fig. 1.11), then this applies even for the short-term fluxes and M/M_{eq}. In finite bath systems, especially if the fractional uptake is greater than 0.7 ($\beta < 0.7$), the effect of various particle size distributions is even more significant than in the case of the infinite bath as discussed above (Cooney et al., 1983). Data on sorptive uptake and desorption in heterogeneous batch systems are challenging to interpret and modeling often requires numerical methods. On the other hand, the sorption and desorption kinetics of organic vapors in different sized polymers have been analyzed in order to determine the grain size distributions (Berens and Huvard, 1981).

1.6 TYPICAL DIFFUSION/DESORPTION TIME SCALES (CHARACTERISTIC TIMES)

If the contaminant release is controlled by diffusion-limited desorption, equilibrium conditions are usually not applicable. As discussed above, the diffusive fluxes of sorbing contaminants over short time periods depend on the square root of the capacity factor (α). Since the sorbed contaminant concentration is linearly proportional to α, more extended time periods are required to remove strongly sorbing compounds as compared to weakly sorbing compounds. This also

applies to particles of different sorption capacities, as long as the effective diffusivities are equal). Fig. 1.11 shows data on the desorption of PAHs from a contaminated sand sample which was taken at a former manufactured gas plant site (Grathwohl et al., 1994). This sand had already been "decontaminated" using on-site wet-mechanical treatment ("soil washing" with surfactants) before the desorption was initiated in laboratory column experiments. Despite the on-site treatment the sand still contained significant amounts of PAHs (60 mg/kg to 100 mg/kg). Depending on the grain size fraction coal tar coatings had been removed from the grain surfaces, but resistant PAHs were still present in the intraparticle pore space.

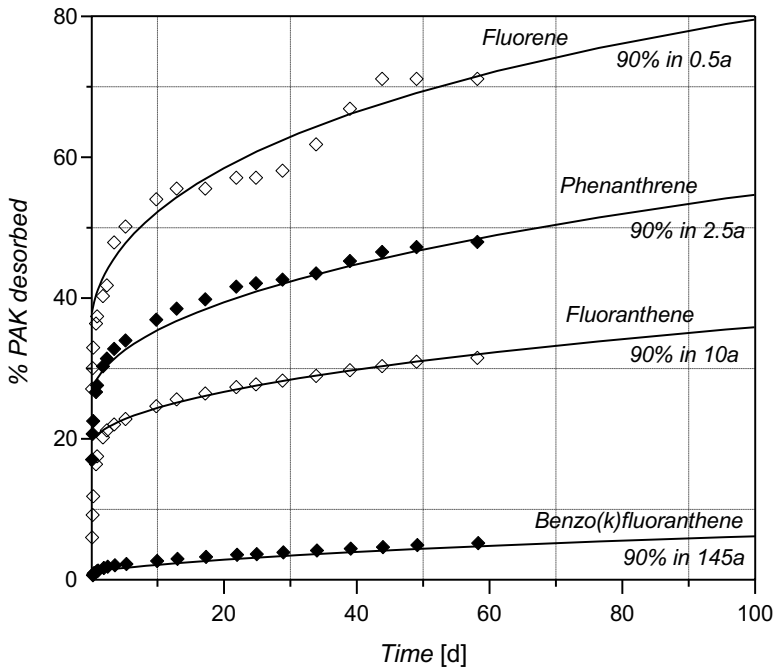

Fig. 1.10: Desorption of PAHs from a contaminated sand from a former gasworks site in column experiments (Grathwohl et al. 1994). Symbols and lines denote data and model (based on Eq.1.5), respectively.

The characteristic time required to remove 90% (t_{90}) and 99% (t_{99}) of the initially existing contaminant (equilibrium conditions) can easily be calculated based on the long-term approximation for M/M_{eq} (eq. 1.5). This approach is valid if the concentration of the mobile zone is close to zero in comparison to the equilibrium concentration (C_{eq}):

$$t_{90} = 0.183\frac{a^2}{D_a}$$

and (1.14)

$$t_{99} = 0.416\frac{a^2}{D_a}$$

The dimensionless times ($D_a\ t/a^2$) for 90% and 99% removal thus are 0.183 and 0.416, respectively. The time for the removal of more than 50% of the contaminant depends on a^2 and D_a. Desorption from coarse grains and removal of highly sorptive compounds will proceed only very slowly. From Fig. 3.2 dimensionless times for the removal of other fractions of the solute mass can be obtained. For non-spherical geometries and non-equilibrium initial conditions see Figs. 1.5 and 1.8, respectively. In Fig. 1.11, the relationships between $D_a\ /a^2$ and the periods

required for removal of 90% and 99% are shown. The diagram also includes some measured data on the desorption of TCE, which is relatively fast compared to that of strongly sorbing compounds such as PAHs. When the contaminant release is due to matrix diffusion (e.g., in fractured rocks where the edges of blocks are larger than 10 cm, or in large confining layers), relatively long periods would be necessary for the remediation of TCE. The removal of strongly sorbing compounds such as PAHs from sands can take decades to centuries.

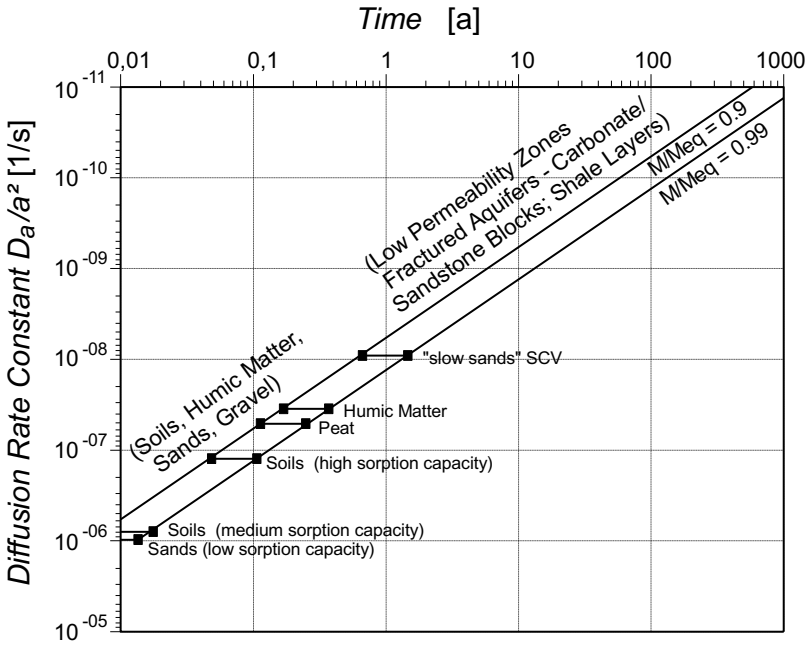

Fig. 1.11: Time to remove 90% and 99% (t_{90}/t_{99}) of the contaminant (M/M_{eq} = 0.9, 0.99) versus D_a/a^2 (equilibrium at t = 0). Symbols and text are based on measured TCE data.

As shown in Section 1.5 long time periods have to be expected for decontamination even when sorption equilibrium had not been reached during the period of contamination. Since the contaminant to some extent still diffuses towards the center of the particle or rock matrix, hysteresis (also called "pseudo"-hysteresis; Miller and Pedit, 1992) develops during decontamination ("the time of decontamination is longer than the time of contamination"). This may explain observations in sorption/desorption experiments of slow desorption after short exposure times which were erroneously attributed to irreversible sorption (Ditoro and Horzempa, 1982; Kan et al., 1994). Fig. 1.7 shows an example of calculated concentration profiles in a sphere when desorption starts before equilibrium was reached.

2. DIFFUSION LIMITED SORPTION/DESORPTION IN THE FINITE BATH (BATCH EXPERIMENTS)

2.1 ANALYTICAL SOLUTIONS

Batch experiments are often used in order to quantify the dynamics of the sorptive uptake of organics by soils and sediments. These experiments are commonly performed in a well-mixed bath of limited volume and an initial spike of solute in the water. The solute concentration in the water then drops from an initial high concentration to a lower concentration at equilibrium. If the particles are free of solute initially, the following initial and boundary conditions apply ("bath of limited volume"):

$$C = 0 \qquad t = 0 \qquad 0 < r < a$$

$$C = C_{eq} \qquad t = \infty \qquad r = a$$

$$\partial C/\partial r = 0 \qquad t > 0 \qquad r = 0$$

The analytical solution (Crank, 1975) of the mass of solute in the sphere after time t (M) relative to the mass in the sphere at equilibrium (M/M_{eq}) is:

$$\frac{M}{M_{eq}} = 1 - \sum_{n=1}^{\infty} \frac{6\beta(\beta+1)}{9 + 9\beta + q_n^2\beta^2} \exp\left[-q_n^2 \frac{D_a}{a^2} t\right] \tag{2.1}$$

The q_ns are the non-zero roots of:

$$\tan q_n = \frac{3q_n}{3 + \beta q_n^2} \tag{2.2}$$

β denotes the ratio of the mass of solute dissolved in the free aqueous phase $M_{w,eq}$ [M] to the mass in the particles (sorbed and dissolved in the intraparticle pore space ε) $M_{s,eq}$ [M] under equilibrium conditions:

$$\beta = \frac{M_{w,eq}}{M_{s,eq}} = \frac{V_w}{m_d\left(K_d + \frac{\varepsilon}{\rho_p}\right)} \approx \frac{V_w}{m_d K_d} \tag{2.3}$$

V_w and m_d and ρ_p denote the volume of water in the batch reactor [L^3] and the dry mass of the solids and the bulk density of the particle. The approximation neglects the intraparticle porosity (ε/ρ_p is commonly much smaller than K_d). Often the fractional uptake or the fraction dissolved at equilibrium are used:

$$f_{sorbed} = \frac{M_{s,eq}}{M_{w,eq} + M_{s,eq}} = \frac{1}{1+\beta} \approx \frac{1}{1 + \frac{V_w}{m_d K_d}}$$

$$f_{dissolved} = \frac{M_{w,eq}}{M_{w,eq} + M_{s,eq}} = \frac{1}{1 + \frac{1}{\beta}} \approx \frac{1}{1 + K_d \frac{m_d}{V_w}} \tag{2.4}$$

If ε/ρ_p in eq. 2.3 is neglected, then K_d denotes a bulk distribution coefficient between inter-particle water (e.g., mobile phase) and solids as well as intra-particle water (e.g., immobile phase): $K_{d,bulk} = K_d + \varepsilon/\rho_p$. The ratio V_w / m_d represents the liquid to solid ratio LS [L^3 M^{-1}] in the batch reactor which in a packed bed (porous media) corresponds to ratio of porosity n and bulk density of the solids in the system ρ [M L^{-3}] assuming a density of water of 1 this equals the water content):

$$LS = \frac{V_w}{m_d} = \frac{n}{\rho} \tag{2.5}$$

Note, that assuming a density of water of 1 g cm^{-3}, *LS* simply represents the gravimetric water content; n is the porosity in a water saturated system (intergranular water), in unsaturated systems the volumetric water content is used (θ); the bulk density $\rho = (1 - n)\ \rho_p$

If K_d is larger than ε/ρ_p then β simply denotes the liquid solid ratio divided by K_d as already used in first order kinetics in the finite bath. For diffusion into solid particles (polymers) ε is zero. If K_d is zero, then ε/ρ_p represents a "K_d " of the solute present in intraparticle pore water.

For large values of n (> 50) or large β, the q_ns in Eqs. 2.1 and 2.2 approach $n \cdot \pi$. If β approaches infinity ("infinite bath") Eq. 2.1 equals Eq. 1.5. For short time periods ($D_a t / a^2 < 0.01$) a large number of terms (n > 50) is necessary in Eq. 2.1 and the application of a ***short-term approximation*** may be convenient. If t is small enough, 2.1 can be reduced to (Barrer, 1978):

$$\frac{M}{M_{eq}} = 6\left(1 + \frac{1}{\beta}\right)\sqrt{\frac{D_a t}{\pi\, a^2}} = 6\left(1 + K_d \frac{m_d}{V_w}\right)\sqrt{\frac{D_a t}{\pi a^2}}$$

$$\text{for } K_d \frac{m_d}{V_w} \gg 1 \tag{2.6}$$

$$\frac{M}{M_{eq}} \approx 6\ \frac{m_d}{V_w}\sqrt{\frac{D_e\ K_d\ t}{\pi\ \rho\ a^2}}$$

Note, this is based on the bulk distribution coefficient; α in the apparent diffusion coefficient then is just $K_d\ \rho$ ($D_a = D_e/(K_d\ \rho)$. At early times the approach to equilibrium gets faster with increasing K_d.

The corresponding short-term flux is given by the time derivative:

$$\frac{F}{M_{eq}} = 3\left(1 + K_d \frac{m_d}{V_w}\right)\sqrt{\frac{D_a}{\pi a^2}}\ \frac{1}{\sqrt{t}} \tag{2.7}$$

Figure 2.1 shows M/M_{eq} calculated by Eqs. 2.1 and 2.6. With increasing values of β the time range where the simple short-term approximation may be applied becomes smaller and smaller.

The approximations for short time periods for F show that for small values of β (β < 1; f < 0.5) the initial rate of sorptive uptake is higher than in the case of an infinite bath (β → ∞). This is because a relatively high initial aqueous concentration in the finite bath is necessary in order to reach the same M_{eq} as in an infinite bath and this results in high initial concentration gradients (= high sorption rates) at low values of β.

2.2 NON-EQUILIBRIUM "APPARENT" DISTRIBUTION COEFFICIENTS

The sorptive uptake under non-equilibrium conditions can be expressed as the apparent distribution coefficient $K_{d,a}$ relative to the equilibrium K_d:

$$\frac{K_{d,a}}{K_d} = \frac{\beta}{\frac{1+\beta}{M/M_{eq}} - 1} \approx \frac{1}{\frac{1 + K_d \frac{m_d}{V_w}}{M/M_{eq}} - K_d \frac{m_d}{V_w}} \tag{2.8}$$

Realizing that M/M_{eq} in the sorptive uptake mode equals $C_s/C_{s,eq}$ and replacing $1/\beta$ approximately by $K_d\, m_d/V_w$ (as mentioned $K_d << \varepsilon/\rho_p$ and K_d now denotes the bulk K_d) we get:

$$\frac{M}{M_{eq}} = \frac{C_s}{C_{s,eq}} = 6\left(1 + \frac{1}{\beta}\right)\sqrt{\frac{D_a t}{\pi\, a^2}} \approx \frac{6}{\rho}\left(\frac{1}{K_d} + \frac{m_d}{V_w}\right)\sqrt{\frac{D_e\, K_d\, \rho\, t}{\pi\, a^2}} \tag{2.9}$$

$C_s/C_{s,eq}$ may be evaluated based on the mass balance (mass conservation):

$$C_s m_d + C_w V_w = C_{s,eq} m_d + C_{w,eq} V_w$$

Replacing C_w with $\frac{C_s}{K_{d,a}}$ and $C_{w,\mathrm{eq}}$ with $\frac{C_{s,eq}}{K_d}$ leads to:

$$C_s m_d + \frac{C_s}{K_{d,a}} V_w = C_{s,eq} m_d + \frac{C_{s,eq}}{K_d} V_w$$

$$C_s\left(m_d + \frac{V_w}{K_{d,a}}\right) = C_{s,eq}\left(m_d + \frac{V_w}{K_d}\right) \tag{2.10}$$

thus

$$\frac{C_s}{C_{s,eq}} = \frac{\left(m_d + \frac{V_w}{K_d}\right)}{\left(m_d + \frac{V_w}{K_{d,a}}\right)} = \frac{K_{d,a}\left(K_d \frac{m_d}{V_w} + 1\right)}{K_d\left(K_{d,a} \frac{m_d}{V_w} + 1\right)}$$

with that eq. 2.9 becomes:

$$\frac{C_s}{C_{s,eq}} = \frac{K_{d,a}\left(K_d \frac{m_d}{V_w} + 1\right)}{K_d\left(K_{d,a} \frac{m_d}{V_w} + 1\right)} = 6\left(K_d \frac{m_d}{V_w} + 1\right)\sqrt{\frac{D_a t}{\pi a^2}} \tag{2.11}$$

$$\frac{K_{d,a}}{K_d} = 6\left(K_{d,a} \frac{m_d}{V_w} + 1\right)\sqrt{\frac{D_a t}{\pi a^2}}$$

Hence, sorptive uptake expressed as $K_{d,a}/K_d$ is insensitive to different liquid solid ratios at early stage (when $K_{d,a}$ is still very small) and if plotted vs. dimensionless time (Fourier number). In fact the increase of $K_{d,a}/K_d$ in all cases (independent on β) is very similar to M/M_{eq} and as shown in Fig. 2.2 this also holds for longer time periods; in fact $K_{d,a}/K_d$ follows the uptake curve closely for the infinite bath even for different values of β (and is close to M/M_{eq} in the infinite bath). M/M_{eq} (= $C_s/C_{s,eq}$ in sorptive uptake mode) in the finite bath at given time is larger than $K_{d,a}/K_d$ (= C_s/C_w $C_{s,eq}/C_{s,eq}$) because initially C_w is large and for strong sorption $C_{w,eq}$ is small.

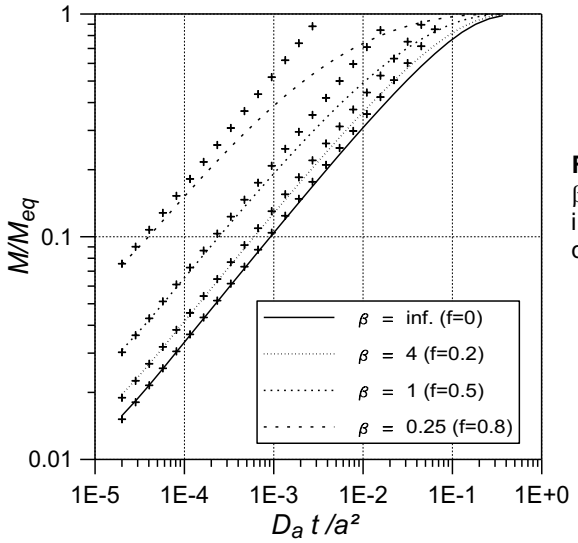

Fig. 2.1: Analytical solutions of M/M_{eq} for different values of β (β → ∞: infinite bath; low β denotes high sorptive uptake, i.e. high K_d and/or high solid to liquid ratios); cross symbols denote the short-term approximations (Eq. 2.6)

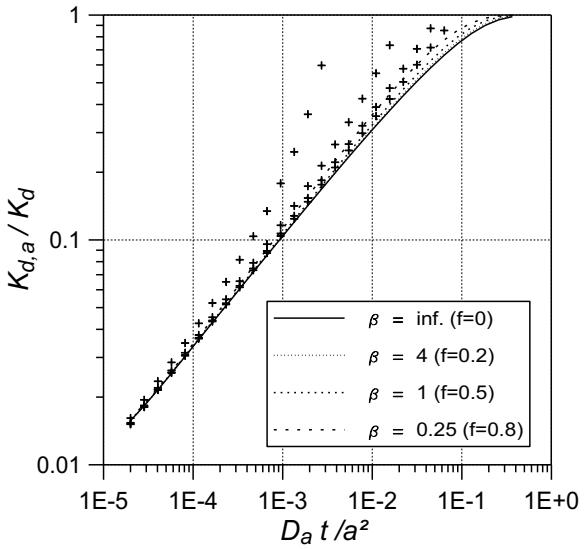

Fig. 2.2: $K_{d,a}/K_d$ versus time for different values of β (β→ ∞: infinite bath) during sorptive uptake; cross symbols denote the short-term approximations (Eq. 2.6, 2.11)

2.3 NON-SPHERICAL GEOMETRIES

Sorptive uptake of a solute by non-spherical particles, e.g. plane sheets (slabs) in a batch sorption experiment of limited volume may be calculated according to Cole (1983):

$$\frac{M}{M_{eq}} = 1 - \sum_{n=1}^{\infty} \frac{2\beta(\beta+1)}{1+\beta+q_n^2\beta^2} \exp\left[-q_n^2 \frac{D_a}{d^2} t\right] \tag{2.12}$$

where the q_ns, in this case, are given by:

$$\tan q_n = -\beta q_n \tag{2.13}$$

For the higher-order terms in Eq. 2.12 and/or large values of β, the q_ns approach n·π. For a single slab (parallelepiped) in a finite bath, β is defined as:

$$\beta = \frac{V_w}{bcd\rho K_d} \tag{2.14}$$

where $(b\ c\ d\ \rho)/V_w$ denotes again the solid to water ratio in a batch experiment (see Eqs. 2.3 and 2.5).

Approximations of sorptive uptake and desorption in a batch reactor of limited volume for short time periods are also independent of the geometries. This is shown above for the case of the infinite bath and may be expressed as (Barrer, 1978):

$$\frac{M}{M_{eq}} = \frac{2A}{V}\left(\frac{1}{\beta}+1\right)\sqrt{\frac{D_a t}{\pi}} \tag{2.15}$$

The corresponding diffusion rates are easily obtained by the time derivative of Eq. 2.15.

According to Rao and Jessup (1982) non-spherical aggregates such as cubes of edge c can also be represented by spherical aggregates of equivalent volume:

$$\mathrm{a} = \mathrm{c}\left(\frac{4}{3}\pi\right)^{-1/3} \tag{2.16}$$

As the examples in Fig. 1.5 show, the uptake and desorption curves are only affected by the particle geometry for long time periods (if based on the same A/V surface to volume ratios). However, if time is normalized using the radius, diameter or thickness (and not A/V) of a particle, the curves in Fig. 1.4 would also separate also at early times.

Box 2.1. How to relate M/M_{eq} to aqueous concentrations in batch experiments (finite baths)?

M/M_{eq} may be easily converted to concentrations in water during a batch experiment. In a sportive uptake experiment M (the mass diffused into a sphere after time t) is given as the difference between the mass initially in water and the mass in water after time t ($C_{w,ini}\ V_w$ - $C_w\ V_w$); M_{eq} (the mass in the sphere at equilibrium) is the difference between the mass initially in water and the mass in water at equilibrium ($C_{w,ini}\ V_w$ - $C_{w,eq}\ V_w$). M/M_{eq} then simply is (V_w drops out):

$$\frac{M}{M_{eq}} = \frac{C_{w,ini} - C_w}{C_{w,ini} - C_{w,eq}} = \frac{1 - \frac{C_w}{C_{w,ini}}}{1 - \frac{C_{w,eq}}{C_{w,ini}}}$$

Realizing (again based on mass balance considerations, but neglecting ε/ρ_p), that

$$\frac{C_{w,eq}}{C_{w,ini}} = \frac{C_{w,eq}}{\frac{C_{w,eq}V_w + C_{s,eq}m_d}{V_w}} = \frac{C_{w,eq}}{C_{w,eq} + C_{w,eq}K_d\frac{m_d}{V_W}} = \frac{1}{1 + K_d\frac{m_d}{V_w}}$$

the short-term approximation for sorptive uptake (eq. 2.9) becomes:

$$1 - \frac{C_w}{C_{w,ini}} = 6\left(1 + K_d\frac{m_d}{V_w}\right)\sqrt{\frac{D_a t}{\pi a^2}}\left(1 - \frac{C_{w,eq}}{C_{w,ini}}\right)$$

$$\frac{C_w}{C_{w,ini}} = 1 - \left(6\left(1 + K_d\frac{m_d}{V_w}\right)\sqrt{\frac{D_a t}{\pi a^2}}\left(1 - \frac{1}{1 + K_d\frac{m_d}{V_w}}\right)\right)$$

$$\textbf{and finally: } \frac{C_w}{C_{w,ini}} = 1 - 6\sqrt{\frac{D_a t}{\pi a^2}}\left(1 + K_d\frac{m_d}{V_w} - 1\right)$$

The higher $K_d\ m_d\ /\ V_w$ the faster the concentration in water drops.

Alternatively M/M_{eq} may be converted to $C_w/C_{w,eq}$ again based on the mass balance

($C_{w,in}\ V_w = C_{w,eq}\ V_w + K_d\ C_{w,eq}\ V_w$):

$$\frac{M}{M_{eq}} = \frac{C_{w,eq}V_w + K_dC_{w,eq}m_d - C_wV_w}{C_{w,eq}V_w + K_dC_{w,eq}m_d - C_{w,eq}V_w} = \frac{C_{w,eq}\left(1 + K_d\frac{m_d}{V_w}\right) - C_w}{K_dC_{w,eq}\frac{m_d}{V_w}} = \frac{\left(1 + K_d\frac{m_d}{V_w}\right)}{K_d\frac{m_d}{V_w}} - \frac{C_w}{C_{w,eq}K_d\frac{m_d}{V_w}}$$

the short-term approximation for sorptive uptake (eq. 2.9) now becomes:

$$\left(1 + K_d\frac{m_d}{V_w}\right) - \frac{C_w}{C_{w,eq}} = 6\left(1 + K_d\frac{m_d}{V_w}\right)\sqrt{\frac{D_a t}{\pi a^2}}\left(K_d\frac{m_d}{V_w}\right)$$

and finally:

$$\frac{C_w}{C_{w,eq}} = \left(1 + K_d\frac{m_d}{V_w}\right)\left(1 - 6\sqrt{\frac{D_a t}{\pi a^2}}\left(K_d\frac{m_d}{V_w}\right)\right)$$

At $t = 0$, C_w is R (= 1+ $K_d\ m_d\ /\ V_w$) times higher than $C_{w,eq}$. In the desorption mode M/M_{eq} is equal to $C_w/C_{w,eq}$ (M and M_{eq} denote now the mass diffused out of a sphere after time t and after equilibrium was achieved) and the short term approximation is just:

$$\frac{C_w}{C_{w,eq}} = 6\left(1 + K_d\frac{m_d}{V_w}\right)\sqrt{\frac{D_a t}{\pi a^2}}$$

Under equilibrium conditions $C_{w,eq}$ is by ($V_w\ /\ m_d + K_d$) smaller than the initial concentration in the solids.

2.4 SHORT TERM APPROXIMATION FOR INTRAPARTICLE DIFFUSION – CHARACTERISTIC TIMES

The film diffusion (first order) model can be extended by assuming an internal mass transfer resistance such as intra-particle pore diffusion. The mass transfer coefficient k may be expressed as D_e/δ, where D_e is the effective diffusion coefficient in the porous particle ($\approx D_{aq}\ \varepsilon^2$) and δ the mean square displacement (= diffusion distance) which grows with the square root of time. The concentration in water during desorption in a batch experiment (equals C_s in a sorptive uptake experiment) is:

$$\frac{\partial C_w}{\partial t} = \frac{D_e}{\delta}\, A^o \left(\frac{\mathrm{V_w}}{K_d\, m_d} + 1\right)\left(C_{w,eq} - C_w\right) \tag{2.17}$$

$$\approx \frac{D_e}{\sqrt{\pi D_a\, t}}\, A^o \left(\frac{\mathrm{V_w}}{K_d\, m_d} + 1\right)\left(C_{w,eq} - C_w\right)$$

$$\approx \sqrt{\frac{D_a}{\pi\, t}}\, \frac{K_d\, \rho\, 3\, m_d}{\rho\, a\, \mathrm{V_w}} \left(\frac{\mathrm{V_w}}{K_d\, m_d} + 1\right)\left(C_{w,eq} - C_w\right)$$

$$= \sqrt{\frac{D_a}{\pi\, t}}\, \frac{3}{a} \left(1 + K_d \frac{m_d}{V_w}\right)\left(C_{w,eq} - C_w\right)$$

D_a is the apparent diffusion coefficient (= $D_e/(\varepsilon + K_d\, \rho_p)$); the approximation is based on $\varepsilon << K_d\, \rho_p$ ($D_e \approx D_a\, K_d\, \rho_p$).

$$\int_0^{C_w} \frac{\partial C_w}{C_{w,eq} - C_w} = \int_0^{t} \sqrt{\frac{D_a}{\pi\, t}}\, \frac{3}{a} \left(1 + K_d \frac{m_d}{V_w}\right) dt \tag{2.18}$$

$$-\ln\left(C_{w,eq} - C_w\right) + \ln\left(C_{w,eq}\right) = 2\sqrt{\frac{D_a\, t}{\pi}}\, \frac{3}{a} \left(1 + K_d \frac{m_d}{V_w}\right)$$

$$\ln\left(\frac{C_{w,eq} - C_w}{C_{w,eq}}\right) = \ln\left(1 - \frac{C_w}{C_{w,eq}}\right) = -2\sqrt{\frac{D_a\, t}{\pi}}\, \frac{3}{a} \left(1 + K_d \frac{m_d}{V_w}\right)$$

$$\frac{C_w}{C_{w,eq}} = 1 - \exp\left(-6\sqrt{\frac{D_a\, t}{\pi\, a^2}} \left(1 + K_d \frac{m_d}{V_w}\right)\right)$$

This is a relatively simple and thus a useful approximation for sorptive uptake in a batch experiment (which otherwise is quite tedious to handle). For small agruments in the exponential function it reduuces to square root of time approximation for sorption kinetics (because 1-exp(-x) ≈ x for x < 0.2) which holds only for low $C_w/C_{w,eq}$ or M/M_{eq} (< 0.5). In contrast to that, eq. 2.18 still holds for large values of equilibration (> 80%). Finally the diffusion distance becomes larger than the grain radius, which is unrealistic (in that case the appropriate first order approximation may be used). The solution for early time intraparticle diffusion (very early times $C_w << C_{w,eq}$) may be obtained upon integration assuming C_w stays practically 0 during early times:

$$\int_0^{C_w} \frac{\partial C_w}{C_{w,eq}} = \int_0^t \sqrt{\frac{D_a}{\pi\, t}}\, \frac{3}{a} \left(1 + K_d \frac{m_d}{V_w}\right) dt \tag{2.19}$$

$$\frac{C_w}{C_{w,eq}} = 2\sqrt{\frac{D_a\, t}{\pi}}\, \frac{3}{a} \left(1 + K_d \frac{m_d}{V_w}\right) = 6 \left(1 + K_d \frac{m_d}{V_w}\right) \sqrt{\frac{D_a\, t}{\pi\, a^2}}$$

For large K_d (and/or large m_d/V_w) values we may use again:

$$\frac{C_w}{C_{w,eq}} \approx 6\, \frac{m_d}{V_w} \sqrt{\frac{K_d\, D_e\, t}{\pi\, \rho\, a^2}} \tag{2.20}$$

which is the early time approximation for diffusion into an infinite sorbent.

Characteristic times for intraparticle diffusion may be easily obtained assuming an argument of -1 in eq. 2.18 which corresponds to $C_w/C_{w,eq}$ of 0.63:

$$t_{0.63} = \frac{1}{\left(1 + K_d \frac{m_d}{V_w}\right)^2} \frac{\pi\, a^2}{36\, D_a} \tag{2.21}$$

This approximation holds for reasonably well especially for small values of $K_d\, m_d/V_w$ (approaching the infinite bath) until values of 4 are reached. The smaller $C_w/C_{w,eq}$ the better the fit. If we evaluate eq. 2.21 we get:

$$t_{0.63} = \frac{\pi\, a^2}{36\, D_a \left(1 + 2\, K_d \frac{m_d}{V_w} + \left(K_d \frac{m_d}{V_w}\right)^2\right)} \tag{2.22}$$

The apparent intraparticle diffusion coefficient D_a may be estimated according to literature (Grathwohl, 1998; Rügner et al., 1999; Boving and Grathwohl, 2001):

$$D_a = \frac{D_{aq}\, \varepsilon^2}{\varepsilon + K_d\, \rho} \approx \frac{D_{aq}\, \varepsilon^2}{K_d\, \rho} \tag{2.23}$$

ρ denotes here the bulk density of the particle. Assuming an intraparticle porosity of approx. 5% ($\varepsilon^2 = 0.0025$) and $K_d\, \rho >> \varepsilon$ we get:

$$D_a \approx \frac{D_{aq}}{400\, K_d\, \rho} \tag{2.24}$$

With that we get:

$$t_{0.63} = \frac{\pi\, a^2}{\frac{36\, D_{aq}}{400\, a^2\, K_d\, \rho} \left(1 + 2\, K_d \frac{m_d}{V_w} + \left(K_d \frac{m_d}{V_w}\right)^2\right)} = \frac{35\, \rho\, a^2}{D_{aq} \left(\frac{1}{K_d} + 2\frac{m_d}{V_w} + K_d \left(\frac{m_d}{V_w}\right)^2\right)} \tag{2.25}$$

Note, that now (because of the definition of D_a in eq. 2.24) with intraparticle pore diffusion a **maximum equilibration time is reached for K_d = LS** (β = 1; the term in parenthesis then becomes $4/LS$). Thus, this maximum equilibration time becomes longer with increasing LS

(decreasing m_d/V_w) and increasing grain size squared. If K_d becomes larger than LS then equilibration accelerates because at higher K_d values the solid phase now has a higher capacity for the solute and a lower fraction has to diffuse into the water for equilibration (conversely at low K_d or high LS all solute has to diffuse into the water). Fig. 2.2 shows $t_{0.63}$ as a function of K_d and a.

Instead of characteristic times derived from the short term approximation (eqs. 2.21) the literature also reports other approximation (e.g. the "Glückauf equation"):

$$t_{0.63} = \frac{1}{\left(1 + K_d \frac{m_d}{V_w}\right)} \frac{a^2}{15\, D_a} \tag{2.26}$$

Note that here the term in parenthesis is not squared and 15 replaces $36/\pi$ (= 11.5). As Fig. 2.3 shows this is only valid to intermediate vlaues of $K_d\, m_d/V_w$ (then $72/\pi$ =22.9 would be expected). Table 2.1 finally shows a comparison of characteristic time of different mass transfer models.

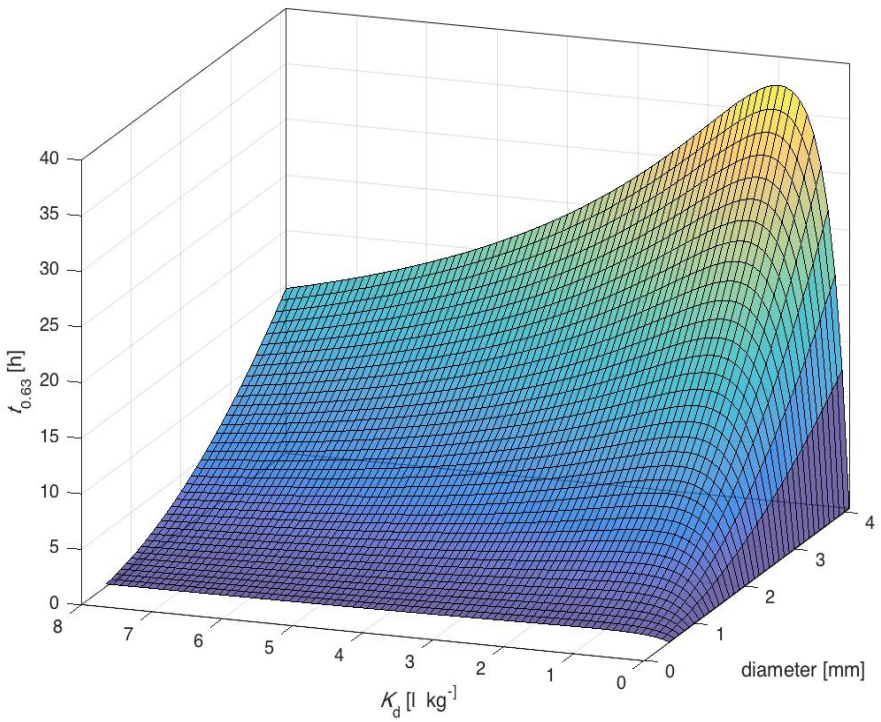

Fig. 2.2: Characteristic time for 63% equilibration $t_{0.63}$ as a function of K_d and particle size. Liquid-solid ratio = 1; note, the maximum time at K_d =1 (= LS).

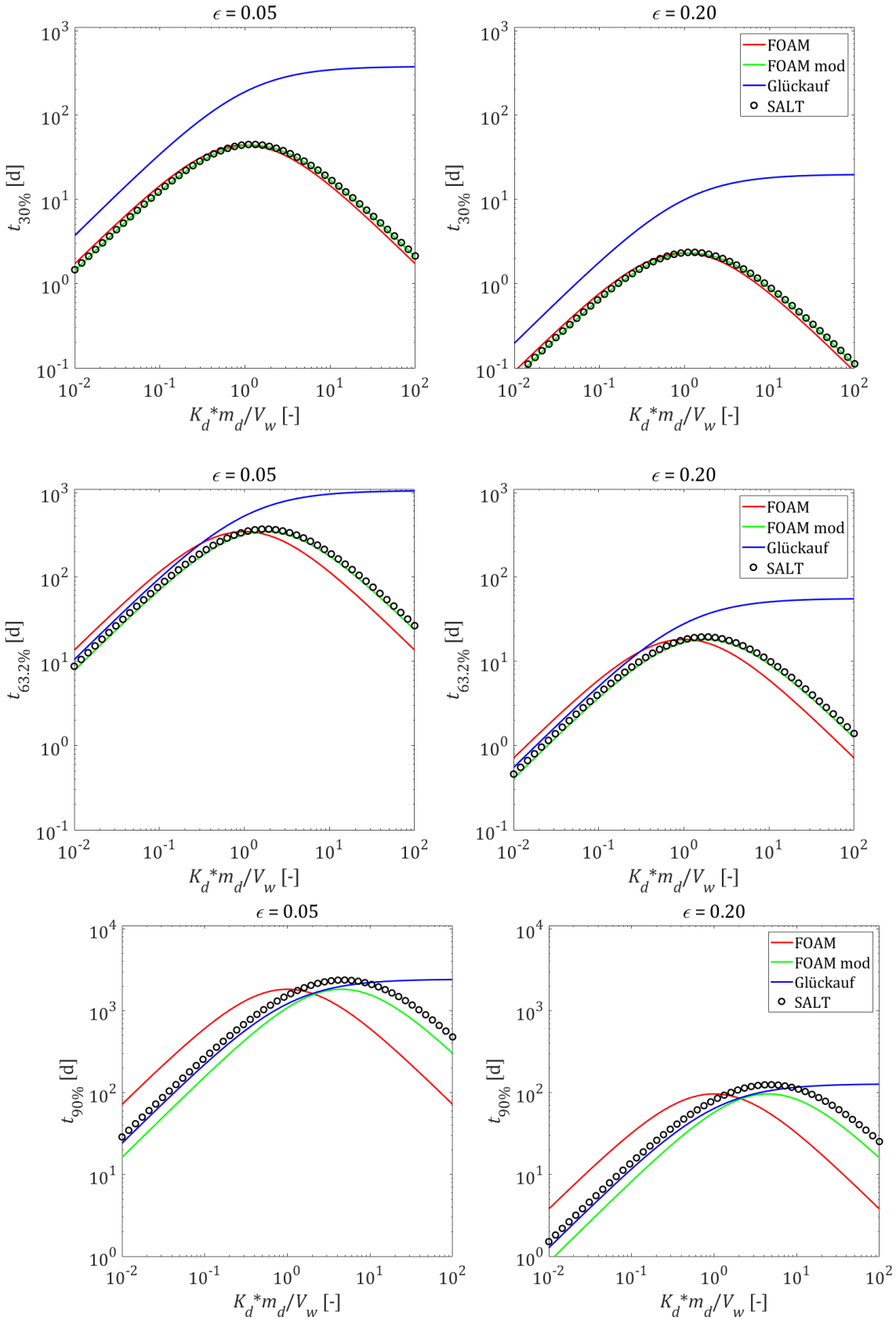

Fig. 2.3. Comparison of approximations for 10%, 63% and 90% equilibration time ($t_{10\%}, t_{63.2\%}, t_{90\%}$) versus $K_d m_d/V_w$ from "square root" of approximations (red lines), fitted approximations (green, multiplication of K_d in eq. 2.25 by 0.85, 0.57 and 0.22 for $t_{10\%}, t_{63.2\%}, t_{90\%}$; this correction factor can be fairly well predicted by 1- $(M/M_{eq})^2$), Glückauf's solution (blue lines) as well as the 'true' equilibration time from the semi-analytical analytical solution (black circles: SALT) for two porosities (ε) left and right; from Binlong Liu, 2024 (d = 2 mm, D_{aq} = 7.5× 10^{-10} m^2 s^{-1}, ρ_s = 2.7 kg L^{-1}).

Box 2.2. Why are time scales for sorption/desorption so different depending on the boundary conditions?

Time scales for sorption/desorption in the infinite bath increase with increasing sorption coefficient (K_d) regardless, whether an external film or intra-particle diffusion limit kinetics (e.g., during desorption the sorbate will be released completely, which takes more time at higher sorption capacities; during sorptive uptake more solute mass has to be sorbed). In the finite bath (bottle, vials etc.) the question is quite different, e.g. how fast does the water equilibrate with the solid during sorption/desorption. For film diffusion, kinetics are described by:

$$\frac{M}{M_{eq}} = 1 - \exp\left(-\frac{D_{aq}}{\delta}\frac{3}{\rho\, a}\left(\frac{m_d}{V_w} + \frac{1}{K_d}\right)t\right)$$

For small K_d values (< m_d/V_w) equilibration time increases with increasing K_d (same as in the infinite bath) but with increasing time K_d drops out and equilibration becomes independent on K_d (and thus becomes almost independent of the properties of the compound) and only depends on the solid to liquid ratio. In sorptive uptake this means that concentrations in water drop to very small values and it does not matter whether 90%, 99% or more of the initial solute is sorbed. During the release of a solute only very little will desorb until the equilibrium concentration is water is reached. This will be accelerated if the solid to water ratio increases (m_d/V_w) – if the water volume is small only very little of the solute is required to achieve the equilibrium concentration in water. Large m_d/V_w ratios coincide with large surface to volume ratios.

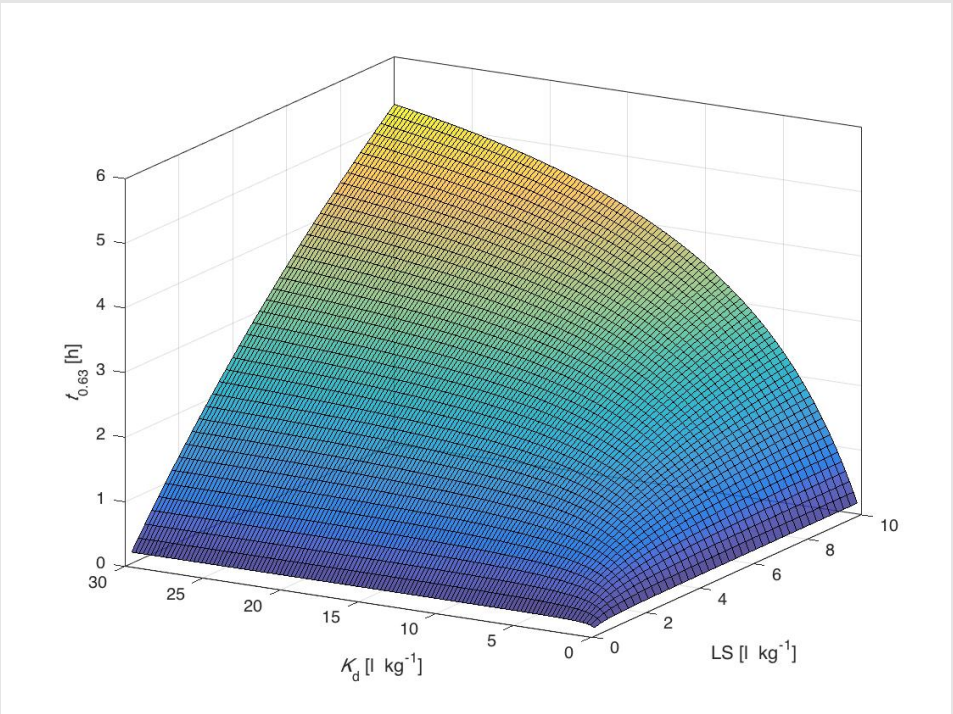

d = 2 mm; Sh =1; note $LS = V_w/m_d$

For intra-particle diffusion in a batch system the short-term approximation is:

$$\frac{M}{M_{eq}} = 1 - \exp\left(-6\left(1 + K_d\frac{m_d}{V_w}\right)\sqrt{\frac{D_{particle}\, t}{\pi\, a^2}}\right)$$

At large m_d/V_w sorptive uptake or desorption in the finite bath is relatively rapid at early times. This has to do with the change of the concentration gradients inside the particles at early times, which are initially very steep and thus solute fluxes are extremely high leading to fast changes in aqueous concentrations at early times (the system "remembers" that at late times).

Fore intra-particle pore diffusion, the dependence on K_d is more complicated because of retardation of the solute within the pores:

$$\frac{M}{M_{eq}} = 1 - \exp\left(-6\left(1 + K_d\frac{m_d}{V_w}\right)\sqrt{\frac{D_a\, t}{\pi\, a^2}}\right) = 1 - \exp\left(-6\left(1 + K_d\frac{m_d}{V_w}\right)\sqrt{\frac{D_e\, t}{(\varepsilon + K_d\,\rho)\,\pi\, a^2}}\right)$$

Again, kinetics gets accelerated with increasing m_d/V_w. (squared at high K_d). Note, that now a global maximum for the equilibration time exists, because K_d now also appears in the denominator of the square root. The maximum equilibration time is reached for $K_d = LS$. If K_d becomes higher than LS, which in batch experiments typically is the case (to minimize errors in the mass balance calculation), then equilibrium is reached slightly faster with increasing sorption. In general, equilibration time increases with increasing LS, but at very small K_d (<< LS) the equilibration time becomes finally independent on LS. As shown below and in Fig. 2.2. increasing LS (or decreasing m_d/V_w.) leads to a strong increase in equilibration time and finally LS is as important as the grains size.

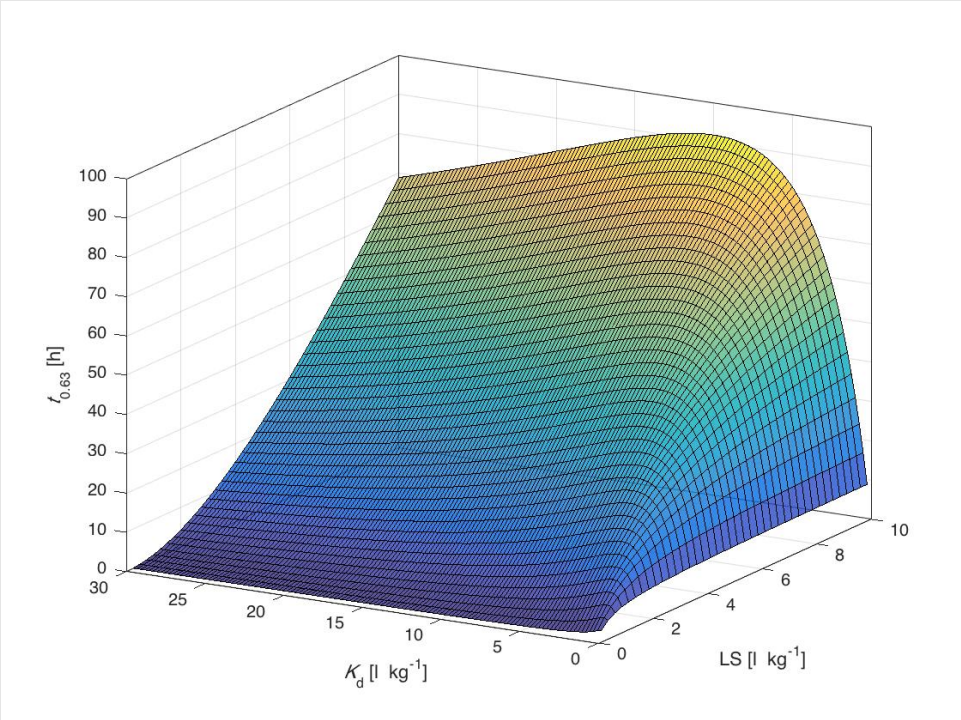

d = 2 mm; $LS = V_w/m_d$; note the maximum time at $K_d = LS$

2.5 APPROXIMATION FOR COUPLED INTRAPARTICLE – FILM DIFFUSION

In reality intraparticle diffusion is coupled to film diffusion (i.e. diffusion trough an external boudary layer). Depending on the compound, particle properites and flow conditions one of the mechanisms may dominate initially; often at long times the mass transfer resitance shifts into the particle (see also the discussion on mass transfer resistance in the column leaching test script). Analogous to the previous chapter an approximation was delopped by Liu et al. (2022) accounting for the external (film diffusion) and internal mass transfer resistance (intraparticle pore diffusion):

$$\frac{\partial M}{\partial t} = \frac{1}{\frac{\delta_p}{D_e} + \frac{\delta_{aq}}{D_{aq}}} \frac{m_d\, 3}{\rho_p\, a\, V_w} \left(1 + \frac{V_w}{m_d\, K_{d,b}}\right) (M_{eq} - M) \tag{2.18}$$

δ_p may be replaced by $\sqrt{\pi D_a\, t}$ (D_a is the apparent diffusion coefficient = $D_e/(\varepsilon + K_d\, \rho_p)$ which for $\varepsilon << K_d\, \rho_p$ becomes $D_e\, /\, K_d\, \rho_p$):

$$\frac{\partial M}{\partial t} = \frac{1}{\sqrt{\frac{\pi\, t}{D_e\, K_{d,b}\, \rho_p}} + \frac{\delta_{aq}}{D_{aq}}} \frac{3}{\rho_p\, a} \left(\frac{m_d}{V_w} + \frac{1}{K_{d,b}}\right) (M_{eq} - M)$$

This can be solved by integration:

$$\frac{M}{M_{eq}} = 1 - \exp\left(-\frac{2}{c^2}\left(b + c\sqrt{t}\right) + \frac{2b}{c^2} \ln\left(b + c\sqrt{t}\right) + \left(\frac{2b}{c^2} - \frac{2b}{c^2} \ln b\right)\right) \tag{2.19}$$

with (and $\delta_{aq} = 2\, a/Sh$):

$$b = \frac{\delta_{aq}}{D_{aq} \frac{3}{\rho_p\, a} \left(\frac{m_d}{V_w} + \frac{1}{K_{d,b}}\right)} = \frac{2\, a^2}{D_{aq} \frac{Sh\, 3}{\rho_p} \left(\frac{m_d}{V_w} + \frac{1}{K_{d,b}}\right)}$$

and:

$$c = \frac{\sqrt{\frac{\pi}{D_e\, K_{d,b}\, \rho_p}}}{\frac{3}{\rho_p\, a} \left(\frac{m_d}{V_w} + \frac{1}{K_{d,b}}\right)}$$

Characteristic times for this case are additive and also shown in Table 2.1.

Table 2.1: Comparison of characteristic times (in []) for film and intraparticle diffusion under finite and infinite bath boundary conditions; approximations (≈) come from $\delta = a$ (Sh = 2) in film diffusion and $D_a \approx \frac{D_{aq}\,\varepsilon^2}{K_d\,\rho}$ (instead of $D_a \approx \frac{D_{aq}\,\varepsilon^2}{\varepsilon + K_d\,\rho}$) for retarded pore diffusion *(parameters in footnote)*.

Finite bath (batch experiments, "bottle")	**Infinite bath ("ocean, atmosphere" $V_w \to \infty$)**	**Finite bath with strong sorbent ($K_d\,m_d/V_w >> 1$)***
Film diffusion: Mass transfer across a stagnant external boundary layer		
$\frac{\rho\,K_d}{\frac{D_{aq}}{\delta}\left(1 + K_d\frac{m_d}{V_w}\right)}\,\frac{a}{3}$ $\approx \frac{\rho\,K_d}{D_{aq}\left(1 + K_d\frac{m_d}{V_w}\right)}\,\frac{a^2}{3}$ $[\mathbf{0.008}]$	$\frac{\rho\,K_d}{\frac{D_{aq}}{\delta}}\,\frac{a}{3}$ $\approx \frac{\rho\,K_d}{D_{aq}}\,\frac{a^2}{3}$ $[\mathbf{0.09}]$	$\frac{\rho}{\frac{D_{aq}}{\delta}\left(\frac{m_d}{V_w}\right)}\,\frac{a}{3}$ $\approx \frac{\rho}{D_{aq}\left(\frac{m_d}{V_w}\right)}\,\frac{a^2}{3}$ $[\mathbf{0.009}]$
(Retarded) intraparticle pore diffusion		
$\frac{\pi\,a^2}{36\,D_a\left(1 + 2\,K_d\frac{m_d}{V_w} + \left(K_d\frac{m_d}{V_w}\right)^2\right)}$ $[\mathbf{0.075}]$ $\approx \frac{\pi}{36}\frac{\rho\,a^2}{D_{aq}\,\varepsilon^2\left(\frac{1}{K_d} + 2\frac{m_d}{V_w} + K_d\left(\frac{m_d}{V_w}\right)^2\right)}$	$\frac{\pi\,a^2}{36\,D_a} = 0.0873\,\frac{a^2}{D_a}$ $[\mathbf{9.1}]$ $\approx \frac{\pi}{36}\,\frac{K_d\,\rho\,a^2}{D_{aq}\,\varepsilon^2}$	$\frac{\pi\,a^2}{36\,D_a\left(K_d\,\frac{m_d}{V_w}\right)^2}$ $[\mathbf{0.091}]$ $\approx \frac{\pi}{36}\frac{\rho\,a^2}{D_{aq}\,\varepsilon^2\,K_d\left(\frac{m_d}{V_w}\right)^2}$
"Glückauf (1/15)" approximation for intraparticle pore diffusion		
$\frac{a^2}{15\,D_a\left(1 + K_d\frac{m_d}{V_w}\right)}$ $[\mathbf{0.631}]$	$\frac{a^2}{15\,D_a} \approx \frac{a^2\,\rho\,K_d}{15\,D_{aq}\,\varepsilon^2}$ $[\mathbf{6.94}]$	$\frac{a^2}{15\,D_{aq}\,\varepsilon^2\left(\frac{m_d}{\rho\,V_w}\right)}$ $[\mathbf{0.694}]$
Coupled intraparticle pore diffusion and film diffusion (eq. 2.19)		
$[\mathbf{0.1}]$	$[\mathbf{9.6}]$	$[\mathbf{0.12}]$
Intraparticle solid diffusion		
$\frac{\pi}{36}\frac{a^2}{D_s\left(1 + 2\,K_d\frac{m_d}{V_w} + \left(K_d\frac{m_d}{V_w}\right)^2\right)}$ $[\mathbf{0.52}]$	$\frac{\pi}{36}\frac{a^2}{D_s} = 0.0873\,\frac{a^2}{D_s}$ $[\mathbf{63}]$	$\frac{\pi}{36}\frac{a^2}{D_s\left(K_d\frac{m_d}{V_w}\right)^2}$ $[\mathbf{0.63}]$

* "infinite" sorbent ("the sorbent takes/keeps it all")

- note, for intraparticle diffusion approximations for t_{ch} exist (e.g., the Glückauf approximation with a linear driving force), which neglect the square term in the parentheses and use 15 instead of $36/\pi$; as shown in Fig. 2.3 this is only valid for $K_d\,m_d/V_w < 1$, see also Liu et al. (2022)
- numbers in parenthesis [] indicate characteristic times in days (radius a = 0.25 mm; D_{aq} = 7×10^{-10} m^2 s^{-1}; ε = 0.05; d_s = 2.65 kg L^{-1}; D_s = 1×10^{-15} m^2 s^{-1}, m_d/V_w = 0.1 kg L^{-1}; K_d = 100 L kg^{-1}; Sh = 2) – note how much longer it takes in the infinite bath
- note, in mixed systems a minor fraction of strongly sorbing particles may "experience" finite bath boundary conditions which would slow down their equilibration tremendously (see Fig. 3.2 and the discussion on heterogeneous system in the script "sorption kinetics first order kinetics")
- film diffusion and intraparticle diffusion are coupled in series, thus the characteristic times are additive

3. PROBLEMS IN FITTING SORPTION KINETICS

3.1 LABORATORY DATA AND DETERMINATION OF DIFFUSION RATE CONSTANTS

In batch experiments on sorptive uptake the sorption coefficient (e.g. K_d) is determined as function of time. Usually, water already containing a given amount of solute (sorbate) is added to the sample or the water is spiked with the solute. By monitoring the decrease of the aqueous concentration of the solute, the amount sorbed is determined. The prerequisite is that the reduction of the aqueous concentration is due solely to sorption of the compound by the soil or sediment sample. If volatilization, degradation (biotic and abiotic) or sorption of the solute onto glass surfaces or liners occurs, a correction term in the mass balance equation is necessary. The decrease of the aqueous concentration due to sorption should be significantly higher than the analytical errors of the measurement of the aqueous concentration (which are typically between 5% and 15%).

For example, the water to solid ratio (volume/mass) required in a batch system to achieve a decrease of the initial aqueous concentration of 50% under equilibrium conditions (50% of the initial mass of solute is sorbed and 50% is in aqueous solution) equals K_d (= V_w/m_d ; V_w and m_d are the volume of water and the dry mass of solids in the batch system, respectively). In well-packed columns with porosities of 0.4, K_d values as low as 0.25 l/kg can be determined with acceptable accuracy. However, in batch experiments, which usually have much higher water to solid ratios than those in column packings, the determination of K_d values below 0.5 l/kg involves significant errors (> 50% error in K_d if an error in the analysis of the aqueous concentration of 15% is assumed).

Soils and sediments are typically heterogeneous which causes difficulties in the evaluation or interpretation of the batch data. Fig. 3.1 shows phenanthrene sorption kinetics in homogeneous lithocomponents separated from aquifer materials, where the single-component diffusion model works. Box. 3.1 shows how desorption can be predicted based on a sorption experiment. Here at early times the fit of the desorption rates in not satisfactory (only the long-term data are predicted). In such cases the models often are incorporate a fraction of instantaneous uptake as shown in Fig. 3.2. To fit measured data, the model of sorptive uptake is extended to incorporate a fraction of instantaneous uptake X_i, which is assumed to reach sorption equilibrium instantaneously. The analytical solution in this case is:

$$\frac{M}{M_{eq}} = (1 - X_i)\left(1 - \sum_{n=1}^{\infty} \frac{6\beta(\beta+1)}{9 + 9\beta + q_n^2\beta^2}\right)\exp\left[-q_n^2 \frac{D_a}{a^2} t\right] + X_i \qquad (3.1)$$

As before β denotes the mass ratio (β) of a solute in the aqueous phase to solute sorbed onto the solids under equilibrium conditions (β = V_w /(m_d (K_d + ε /ρ); how the determination of D_a in a sorptive uptake experiment is sensitive to the K_d values is elaborated in next chapter.

Note that sorptive uptake in heterogeneous samples always results in higher short-term M/M_{eq} than expected for a homogeneous sample. High values of X_i therefore could be an artifact of using a single component model to describe sorption/desorption dynamics in a heterogeneous sample (multicomponent mixtures). The state of equilibrium is difficult to detect while approaching equilibrium (M/M_{eq} = 1) due to analytical limitations (the error in C or M is typical > 5%). For slowly sorbing compounds equilibrium may not be reached during the experiment. Therefore, the

fitting procedure relies on the short-term data (see Fig. 3.2). The sensitivity of fitting parameters can demonstrated from short-term approximation of the analytical solution:

$$\frac{M}{M_{eq}} = (1 - X_i)\, 6 \left(1 + K_{d,b} \frac{m_d}{V_w}\right) \sqrt{\frac{D_a t}{\pi\, a^2}} + X_i$$

for large K_d values ($K_d\, m_d/V_w >> 1$) we get:

$$\frac{M}{M_{eq}} \approx (1 - X_i)\, 6\, K_{d,b} \frac{m_d}{V_w} \sqrt{\frac{D_e t}{\left(K_{d,b}\, \rho\right) \pi\, a^2}} + X_i \qquad (3.2)$$

$$= (1 - X_i)\, 6\, \frac{m_d}{V_w} \sqrt{\frac{D_e\, K_{d,b}\, t}{\rho\, \pi\, a^2}} + X_i$$

For sake of simplicity we use here the bulk sorption coefficient ($K_{d,b} = K_d + \varepsilon\, /\rho$); $(1 - X_i)\, m_d/V_w$ represents the solid/liquid ratio of the slow sorbing particles in the batch system; if this is low sorption or desorption gets slow as well. Since the fraction of slow sorbing particles and their K_d values are often not well known, this introduces large uncertainties in determination of e.g., D_e. Large $K_{d,b}$ values accelerate sorption if monitored in real time which appears opposite to sorption kinetics if plotted as the ratio of the apparent K_d (monitored under nonequilibrium) to the equilibrium K_d (see next chapter). All that shows that interpretation of sorption kinetic data may become really difficult especially in heterogeneous samples. Additionally, shifts in mass transfer mechanisms may occur (typically from film diffusion at early times to intraparticle pore diffusion at late times) and this complicates the mechanistic evaluation of sorption/desorption kinetic data further.

Finally, the short-term solutions are independent of the shape and size of the particles provided that the surface to volume ratio ($A/V = 3/a$ for spheres) of the sorbing particles is known and this also implies that no information on particle shape can be obtained from short-term sorptive uptake experiments.

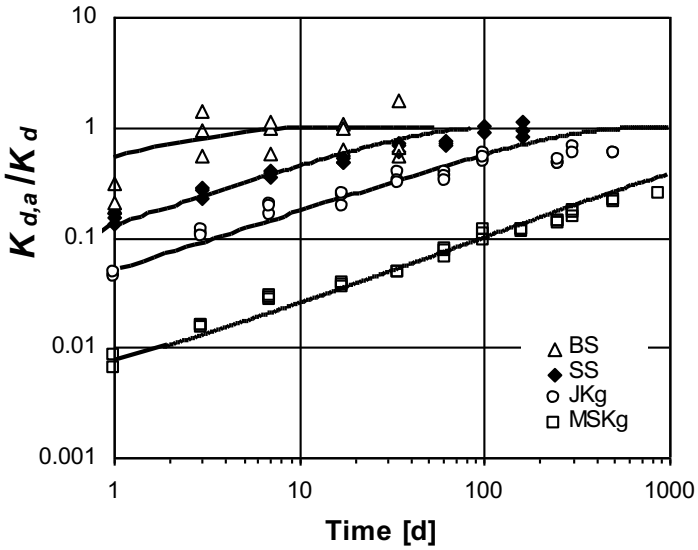

Fig. 3.1: $K_{d,a}/K_d$ for phenanthrene versus time for different samples of rock fragments (BS: Bunter Sandstone; SS: Keuper Sandstone; JK: Jurassic Limestone; MSK: Triassic Limestone). Grain radii 3 mm and 1.4 mm for sandstones and limestones, respectively

Fig. 3.2 illustrates the difficulty in assessing sorption kinetics in batch experiments with heterogeneous samples. In such cases extrapolated times for equilibration (t_{eq}) may differ by orders of magnitude.

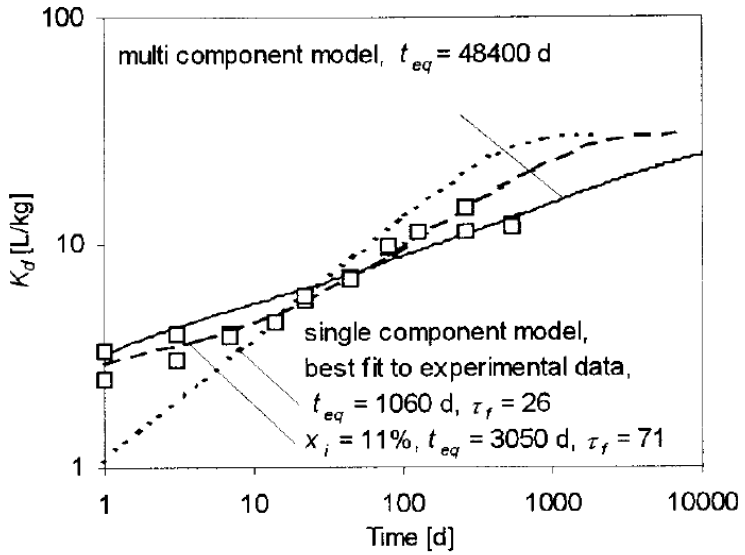

Fig. 3.2: Example for sorptive uptake of phenanthrene in a heterogeneous sand sample (Neckar River, Hirschau) consisting of different grain size fractions (0.063–8 mm) and different lithocomponents. Solid line: Prediction of the sorptive uptake in the heterogeneous sample (pure forward modeling) based on seven grain size fractions and petrographic composition of the grain size fractions > 1 mm (making up 70% of the bulk). Dotted line: Best fit to measured data using a single-component model; t_{eq} is the time to reach 99% of the sorption equilibrium. Dashed line: Best fit as above but including a fraction of instantaneous uptake (x_i). From Kleineidam et al. (1999).

Box 3.1: Column desorption predicted based on a long-term batch sorption experiment. The prediction fits after the time scales are similar. In the column experiment early rates are dominated by dispersion and fast desorption from small grains. The batch approach predicts the desorption rates only for the time scale of more than 3 days. For earlier time periods faster desorbing components have to be introduced in the model (see Fig. 3.2).

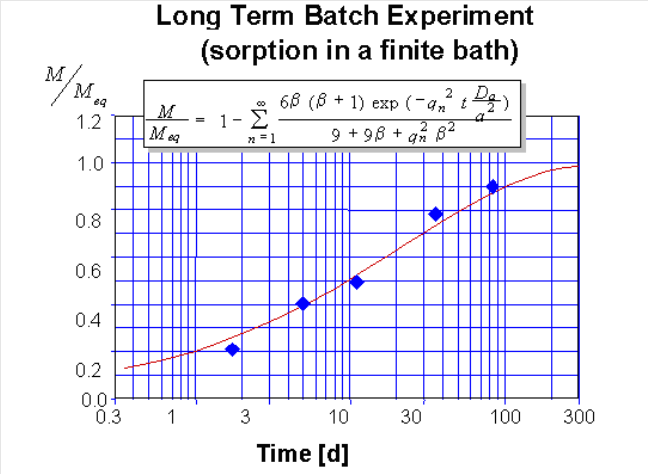

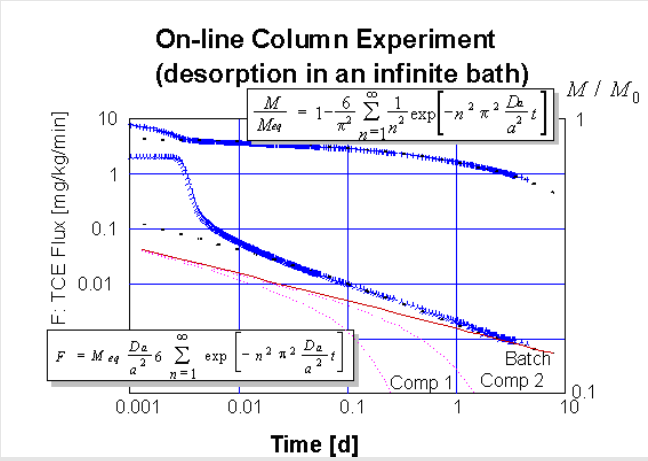

3.2 IDENTIFICATION OF KINETIC MECHANISMS: FILM, INTRAPARTICLE PORE AND SOLID DIFFUSION

As indicated above interpretation of sorption/desorption kinetic data may be difficult and depends on the assumption on the controlling sorption mechanism. This is illustrated for film diffusion, intraparticle pore diffusion and intraparticle solid diffusion in Fig. 3.3 (finite bath).

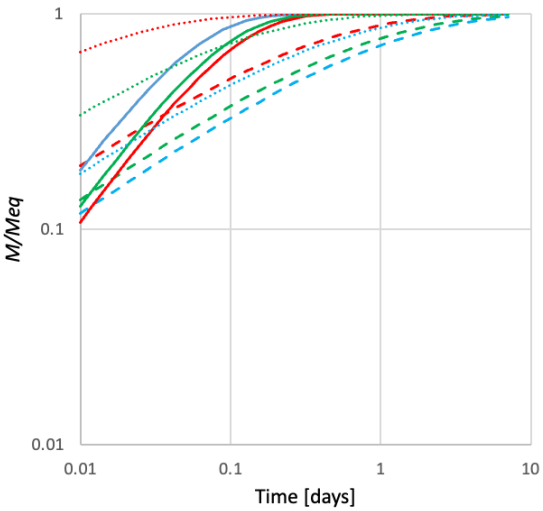

Fig. 3.3: Comparison of film diffusion (FD, solid lines), intraparticle pore diffusion (IPPD, dashed lines) and intraparticle diffusion (IPD, dotted lines) for low (blue), medium (green) and high (red) K_d values (10, 32, 100); m_d/V_w = 0.1.

FD in M/M_{eq} slows down with increasing K_d, opposite in IPPD and IPD.

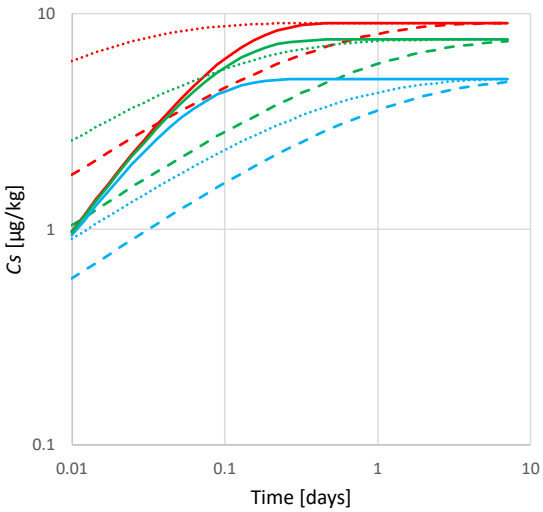

Sorption rates (slopes in C_s) initially are independent on K_d for FD; sorption gets faster with increasing K_d in IPPD and IPD.

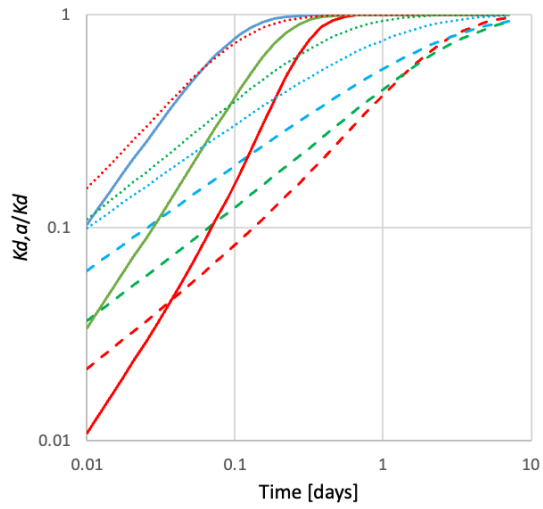

If K_d ratios are monitored large K_d (red) appear slower for FD and IPPD while opposite for IPP ($K_{d,a}$: apparent K_d before equilibrium is reached).

Under infinite bath conditions kinetics again change as illustrated in Fig. 3.4.

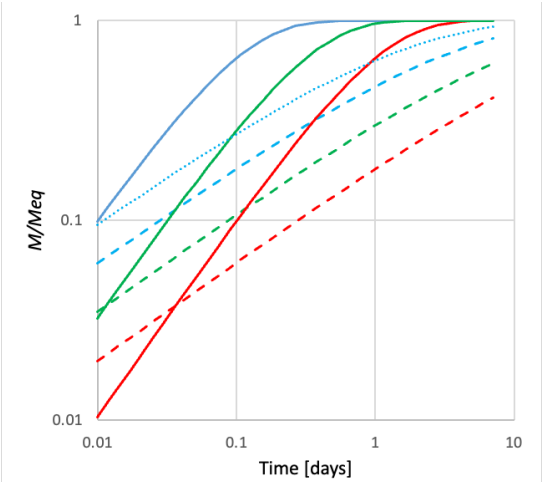

Fig. 3.4: Comparison of film diffusion (FD, solid lines), intraparticle pore diffusion (IPPD, dashed lines) and intraparticle diffusion (IPD, dotted lines) for low (blue), medium (green) and high (red) K_d values (10, 32, 100).

M/M_{eq} for FD and IPPD now slows down with increasing K_d, while curves for IPD overlap.

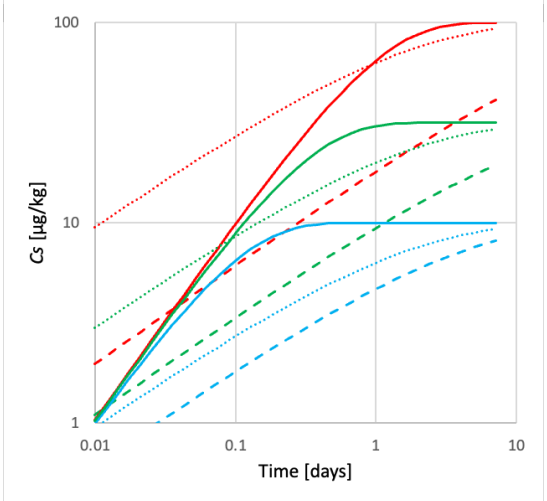

Sorption rates (slopes in C_s) initially again are independent on K_d for FD; concentration increase gets faster with increasing K_d in IPPD and IPD; C_w = 1 µg l^{-1}.

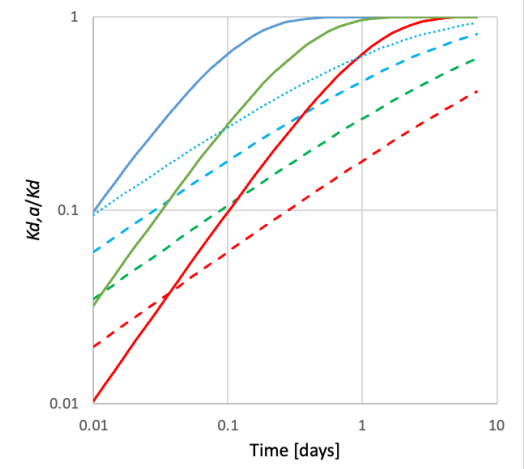

Same as for M/M_{eq} (above); for IPP all lines (K_d -values) overlap.

Note, in all diagrams in Figs. 3.3 and 3.4 at early times film diffusion is slower than intraparticle pore diffusion for large K_d (red) and thus would limit kinetics the first hour and then mass transfer would shift to intraparticle pore diffusion. This shift is independent on m_d/V_w and occurs the earlier the smaller K_d becomes (see Liu et al., 2021).

3.3 FIRST ORDER FITTING FOR DIFFUSION

In most groundwater models where non-equilibrium reactive transport is considered, first-order kinetics are employed to account for sorption/desorption kinetics. Desorption for example is then modeled as a first-order process:

$$\frac{dM_s}{dt} = -\lambda M_s \tag{3.3}$$

where M_s and λ denote the solute mass in the sphere [M or M M^{-1}] and the first order rate coefficient [t^{-1}], respectively. Separation of the variables and the evaluation of the integral yields:

$$\frac{M_s}{M_0} = \exp[-\lambda t] \tag{3.4}$$

where M_s/M_0 denotes the relative solute mass in the sphere at time t. Replacing M_s and M_0 by the mass removed from the sphere after time t and M_{eq}, respectively, yields:

$$\frac{M}{M_{eq}} = 1 - \exp[-\lambda t] \tag{3.5}$$

In order to compare first-order kinetics to diffusive mass transfer, M/M_{eq} in Eq. 3.5 has to be replaced by the corresponding expression for diffusion (e.g.: Eq. 1.2). This determines λ as a function of M/M_{eq} or dimensionless time $(D_a a^2/t)$. Combining Eqs. 3.5 and 1.2 yields:

$$\lambda = -\ln\left[\frac{6}{\pi^2}\sum_{n=1}^{\infty}\frac{1}{n^2}\exp\left[-n^2\pi^2 t\frac{D_a}{a^2}\right]\right]/t \tag{3.6}$$

Eq. 4.4 shows that the diffusion equivalent first-order coefficient depends on time or M/M_{eq}. Determining λ by employing the ***long-term approximation*** for diffusive uptake of a solute by a sphere (first term in Eq. 1.5) yields:

$$\lambda = -\frac{\ln\left(\frac{6}{\pi^2}\right)}{t} + \pi^2\frac{D_a}{a^2} \tag{3.7}$$

As time becomes infinitely large the first term in Eq. 3.7 vanishes and λ approaches $\pi^2 D_a/a^2$. For very ***short periods of time***, λ may be estimated as follows:

$$\lambda = \frac{-\ln\left[1 - 6\sqrt{\frac{D_a t}{a^2\pi}}\right]}{t} \tag{3.8}$$

which for small dimensionless times ($D_a/a^2 < 0.003$, and -ln [1-x] = x for x < 0.1) approaches:

$$\lambda = 6\sqrt{\frac{D_a t}{a^2\pi}} \tag{3.9}$$

Based on the considerations discussed above, λ can be expressed as a function of the diffusion rate constant (Ball, 1989):

$$\lambda = \gamma\frac{D_a}{a^2} \tag{3.10}$$

where γ denotes a proportionality factor that depends on time or M/M_{eq}. For long time periods, γ equals π^2 (see Eq. 3.7). For short time periods γ depends on the inverse of the square root of time:

$$\gamma = 6\sqrt{\frac{a^2}{D_a t \pi}} \tag{3.11}$$

λ and γ are then related to M/M_{eq} and t as follows:

$$\lambda = \frac{M/M_{eq}}{t}; \quad \gamma = M/M_{eq}\frac{a^2}{D_a t} \tag{3.12}$$

Fig. 3.6 shows γ and M/M_{eq} as a function of dimensionless time. Since γ depends on time for short time periods, modeling of diffusion using a first order approach requires a time-varying first order rate coefficient for short time periods as observed in lab experiments (e.g. Connaughton et al., 1993; Croisé et al., 1994). At large time scales, γ approaches π² and diffusion "becomes a first order process".

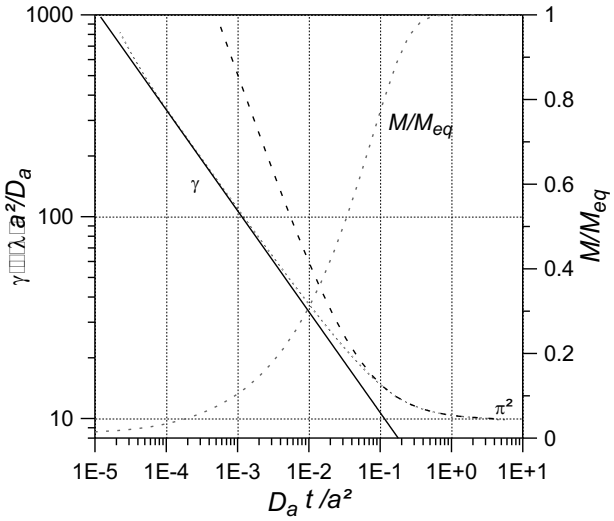

$$\frac{M^{fo}}{M_{eq}} \approx 1 - \exp[-\lambda t]$$

$$\lambda \approx \gamma \frac{D_a}{a^2}$$

γ: Proportionality factor
λ: Rate constant

Fig. 3.6: Proportionality factor γ (left scale) and M/M_{eq} versus dimensionless time (see Eq. 3.6) (right scale). Dotted lines show short (Eq. 3.11) and long-term approximation (based on Eq. 3.7).

3.4 SECOND ORDER FITTING

As shown above first order fitting is not able to simulate transient diffusion processes with a constant rate constant. If first order does not fit data, often second order models are used, which typically are described as follows:

$$C_s = \frac{C_{s,eq}^2 \, K \, t}{1 + K \, C_{s,eq} \, t} \tag{3.13}$$

K is a constant [e.g., in kg μg^{-1} s^{-1}] and $C_{s,eq}^2 \, K$ may be regarded as an initial rate [e.g., in μg kg^{-1} s^{-1}]. For short time periods we expect a linear increase of C_s with time as already observed for first order models; for large time scales equilibrium ($C_{s,eq}$) is approached. Fig. 3.7 shows a comparison of film diffusion and intraparticle pore diffusion with a second order model. In principle the second order model behaves like film diffusion and is not able to simulate intraparticle diffusion.

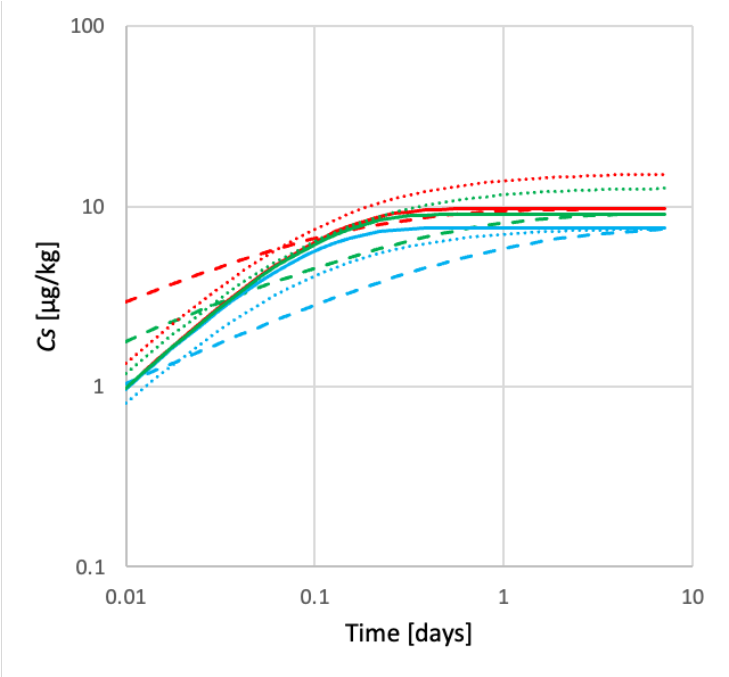

Fig. 3.7: Comparison of film diffusion (FD, solid lines), intraparticle pore diffusion (IPPD, dashed lines) with a second order model (dotted lines) for low (blue), medium (green) and high (red) K_d values (32, 100, 316), m_d/V_w = 0.1; initial rates ($C_{s,eq}^2\ K$) were determined from early time FD data.

4. SOME REFERENCES

Ball, W.P. (1989): Equilibrium partitioning and diffusion rate studies with halogenated organic chemicals and sandy aquifer material. PhD Dissertation, Stanford University, Stanford, California, USA

Ball, W.P., Roberts, P.V. (1991): Long-term sorption of halogenated organic chemicals by aquifer material. 2. Intraparticle diffusion. Environ. Sci. Technol., 25 (7): 1237-1249

Berens, A.R., Huvard, G.S. (1981): Particle size distribution of polymer powders by analysis of sorption kinetics. J. Dispersion Sci. Technol., 2: 359-378

Brusseau, M.L., Jessup, R.E., Rao, P.S.C. (1991): Nonequilibrium sorption of organic chemicals: Elucidation of rate-limiting processes. Environ. Sci. Technol., 25, 134-142

Carslaw, H.S., Jaeger, J.C. 1959: Conduction of heat in solids. Claredon Press, Oxford

Connaughton, D.F., Stedinger, J.R., Lion, L.W., Shuler, M.L. (1993): Description of time-varying desorption kinetics: release of naphthalene from contaminated soils. Environ. Sci. Technol., 27 (12): 2397-2404

Cooney, D.O., Adesanya, B.A., Hines, A.L. (1983): Effect of particle size distribution on adsorption kinetics in stirred batch systems. Chem. Eng. Sci., 38: 1535-1541

Crank, J. (1975): The mathematics of diffusion, 2nd ed.- Oxford, U.K. (University Press)

Croisé, J., Armstrong, J.E., Kaleris, V. (1994): Numerical simulation of rate-limited vapour extraction of volatile compounds in wet sands. In: Dracos, T.H., Stauffer, F. (Eds.): Transport and Reactive Processes in Aquifers, Rotterdam (Balkema), 569-575

Ditoro, D.M., Horzempa, L.M. (1982): Reversible and resistant components of PCB adsorption - desorption isotherms. Environ. Sci. Technol., 16 (9): 594-602

Förstner, U., Grathwohl, P. (2002): Ingenieurgeochemie. Springer, 392 S.

Grathwohl, P. (1998): Diffusion in Natural Porous Media: Contaminant Transport, Sorption/Desorption and Dissolution Kinetics. Kluwer Academic Publishers, Boston, 224 p.

Grathwohl, P., Pyka, W., Merkel, P. (1994): Desorption of organic pollutants (PAHs) from contaminated aquifer material. In: Dracos, T.H., Stauffer, F. (Eds.): Transport and Reactive Processes in Aquifers, Rotterdam (Balkema), p 469-474

Grathwohl, P., Reinhard, M. (1993): Desorption of Trichloroethylene in aquifer material: Rate limitation at the grain scale. Environ. Sci. Technol., 27, 11, 2360-2366

Häfner, F., Sames, D., Voigt, H.-D. (1992): Wärme- und Stofftransport. Springer-Verlag, Berlin, Heidelberg, 626 p.

Kan, A.T., Fu, G., Tomson, M.B (1994): Adsorption/desorption hysteresis in organic pollutant and soil/sediment interaction. Environ. Sci. Technol., 28 (5): 859-867

Kärger, J., Ruthven, D.M. (1992): Diffusion in zeolites and other microporous solids. New York (John Wiley & Sons, Inc.), 605 p

Karickhoff, S.W., Morris, K.R. (1985): Sorption dynamics of hydrophobic pollutants in sediment suspensions. Environmental Toxicology and Chemistry, 4, 469-479

Kleineidam, S., Rügner, H., Grathwohl, P. (1999): Impact of grain scale heterogeneity on slow sorption kinetics. Environ. Tox. Chem., 18, 8, 1673 – 1678. https://doi.org/10.1002/etc.5620180810

Lin, T.-F., Little, J.C., Nazaroff, W.W. (1994): Transport and sorption of volatile organic compounds and water vapor within dry soil grains. Environ. Sci. Technol., 28 (2): 322.330 Madison Wisconsin, USA, pp. 45-80

Liu, B., Finkel, M., Grathwohl, P. (2022): First order approximation for coupled film and intraparticle pore diffusion to model sorption/desorption batch experiments. J. Haz. Mat., 429, 128314 https://doi.org/10.1016/j.jhazmat.2022.128314

Mathews, A.P., Zayas, I.J. (1989): Particle size and shape effects on adsorption rate parameters. J. Environ. Eng., ASCE, 115 (1): 41.55

Miller, C.T., Pedit, J.A. (1992): Use of a reactive surface-diffusion model to describe apparent sorption-desorption hysteresis and abiotic degradation of lindane in a subsurface material. Environ. Sci. Technol., 26 (7): 1417-1427

Pignatello, J.J. (1989): Sorption dynamics of organic compounds in soils and sediments. In: Sawhney B.L. and Brown, K. (Eds.): Reactions and movement of organic chemicals in soils; SSSA Special Publication Number 22,

Schwarzenbach, R.P., Gschwend, P.M:, Imboden, D.M. 1993: Environmental Organic Chemistry. John Wiley & Sons, New York, **Chapter 11.7**

Shonnard, D.R., Bell, R.L., Jackman, A.P. (1993): Effects of nonlinear sorption on the diffusion of benzene and dichloromethane from two air-dry soils. Environ. Sci. Technol., 27 (3): 457-466

Steinberg, M.S., Pignatello, J.J., Sawhney, B.L. (1987): persistence of 1,2-dibromoethane in soils: Entrapment in intraparticle micropores. Environ. Sci. Technol. 21, 1201.1208

Wakao, N., Smith, J.M. (1962): Diffusion in catalyst pellets. Chemical Engineering Science, 17, 825-834

Wu, S., Gschwend, P.M. (1986): Sorption kinetics of hydrophobic organic compounds to natural sediments and soils. Environ Sci. Technol., 20, 717-725